Essays on the Neurophysiological Influences Underpinning Consumer Behavior

by

Steven D. Shaw

A dissertation submitted in partial fulfillment
of the requirements for the degree of
Doctor of Philosophy
(Business Administration)
in the University of Michigan
2021

Doctoral Committee:

Professor Carolyn Yoon, Chair
Associate Professor Joshua Ackerman
Professor Richard Bagozzi
Professor Fred Feinberg
Professor Dave Mayer

Steven D. Shaw

shawsd@umich.edu

ORCID iD: 0000-0002-5556-5629

DEDICATION

And then in the end, it’s family and friends.

ACKNOWLEDGEMENTS

I would like to thank Carolyn Yoon for supporting and believing in me from the day that my application arrived at Michigan, for allowing me to take risks, and for giving me the platform and resources needed to trek through the unknowns of my doctoral journey. You have taught me to keep my eye on the big picture, and the value of perseverance in research endeavors.

I also want to thank Vinod Venkatraman, for your continued research support and valuable feedback that has helped shape my dissertation. Vinod's support, along with help from his team at Temple University, namely, Nicole Henninger and Liz Beard, were invaluable to me, particularly when neuroimaging data collection was halted due to the pandemic.

I am grateful to dissertation committee for the structure you brought to my dissertation, your valuable feedback, and your encouragement. Special thanks to Rick Bagozzi for always bestowing tidbits of wisdom and Fred Feinberg for your positivity and wit throughout the years. I have appreciated the kindness and support from all of the Faculty throughout my time at Ross. Thank you to Rajeev Batra for always keeping me sharp and on my toes. Thank you to Scott Rick for letting me explore wild research ideas and always sharing a laugh. I would also like to thank the Natural Sciences and Engineering Research Council of Canada and the Social Science and Humanities Council of Canada for continually supporting me during my academic career.

I am also grateful for my grad school colleagues and friends at UM. At times, a PhD can be a rather isolating experience; it was always helpful knowing there were others in the same

boat and having good people close by to talk to. Thank you, especially, to Giacomo, Tim, Longxiu, Dana, George, Hedieh, Gwen, Prashant, Ye Fan, Petra, Kate, Rufina, Ada, Brian, Pat, Blake, Guy, Dave, David, Diane, Joey, and Arlene for your comradery, mentorship, and friendship. To the many friends that I have made in Ann Arbor, thank you for the escape from stress and worries, and for listening to me grumble.

To my Canadian friends who have visited me in Ann Arbor for countless football games, rounds of golf, river rides, and nights at 8 Ball, thank you for lifting my spirits by bringing a part of home. Mid, Pete, Trav, Wyatt, Evan, Paul, Tucker, Mike, Russ… keep on given'er and livin'er!

Most importantly, I want to thank my family. Dad, thank you for your patience as I navigated my PhD and for your constant and thoughtful advice. I've admired your work as a professor, and you have inspired my path immensely. Mom, thank you for your encouragement and understanding. Seeing your commitment to teaching has made me a better student and teacher, and helped me throughout my work and service in the program.

Finally, thank you to my one and only partner, Parisa. There are no words that can describe the gratitude I have for your presence in my life.

TABLE OF CONTENTS

LIST OF FIGURES

LIST OF TABLES

ABSTRACT

The broad focus of this dissertation is on consumer neuroscience, aiming to understand how biological factors, such as neural activity, genetic makeup, and other physiological factors, influence consumers' thoughts, attitudes, and decisions. Specifically, this dissertation consists of two essays spanning different biological influences on consumer behavior. In the first essay of my dissertation, I aim to investigate how and under what circumstances neural activity can be used to forecast choices. I provide support for the affective-integration-motivation framework as a foundation for understanding neuroforecasting, and neuroforecast aggregate online dating choices using affective neuroactivity data from the nucleus accumbens. In my second dissertation essay, I discuss the development of a set of Python based tools for gene-level genome-wide association methodology, and demonstrate these tools using single nucleotide polymorph genetic data from ~20,000 individuals from the University of Michigan's Health and Retirement Study. The public availability of these tools will allow researchers to more easily conduct gene-level association methods, empirically test the statistical properties of gene-level approaches, and further develop gene-level association methodologies.

CHAPTER I

Introduction

I am often asked by friends, colleagues, and even strangers, "what does biology have to do with marketing!?". The evolutionary biologist Theodosius Dobzhansky wrote: "nothing in biology makes sense except in the light of evolution". Well, despite the orders of magnitude of difference in timescale and seemingly distal influences of biological influences on our everyday judgments and decisions, our non-human animal foundations do none-the-less influence every aspect of our day-to-day actions. By extension then, nothing in marketing makes sense except in the light of our biology. This is how I approach understanding consumer behavior in the marketplace, and this is why I have chosen to study consumers through a biological level of analysis, using tools and techniques from cognitive neuroscience and genomics.

What follows are two chapters describing the culmination of my research efforts conducted during my time at the Ross School of Business, University of Michigan, Ann Arbor. In the first chapter, I use neuroimaging to develop theory around the fascinating phenomenon of neuroforecasting. Here, by scanning the brain activity of a small group of individuals, I am able to effectively forecast aggregate outcomes for online dating profiles by using affective brain activity in the nucleus accumbens. After providing support for the affective-integration-motivation framework as a foundation for understanding the usefulness of neuroforecasting, I argue that while neuroforecasting can be highly valuable in some contexts, my research findings

could provide a means for marketers to use insights from neuroforecasting to create behavioral variable proxies of neural processes, and use these proxies for making forecasts instead of needing to collect expensive neuroimaging data. Second, I discuss the development of a set of Python-based tools for genome-wide gene-level association. Marketers and economists have only recently garnered access to genetic datasets that may prove useful for understanding genetic influences on consumers in the marketplace. That said, with the rise of massive public (e.g., the UK BioBank) and private (e.g., 23andMe) genetic databases, we have much yet to discover about how our genetic makeup influences complex human behaviors. Here, making a methodological contribution, I describe how these Python tools can be used by researchers to facilitate genetic analysis at the fundamental level of genetic inheritance, the gene.

I hope you enjoy the many pages that follow. And if you don't, that's okay too…

CHAPTER II

Neuroforecasting Aggregate Choice in Online Dating: Forecasting Aggregate Choices From Small Samples Using Neural and Behavioral Measures

The ability to predict the future behavior of individuals or future events (e.g., product success) is of extreme value to society. Although traditional models of choice prediction, which often use past behavior as the basis for prediction, such as revealed preferences (i.e., economic approaches) and behaviorism (i.e., psychological approaches), have proven useful, researchers have now begun to investigate the neural underpinnings of decision-making and choice, and explore the utility of using neural activity data in understanding, predicting, and forecasting choices. Indeed, neural data is evidenced to improve on behavioral forecasts of choice (Bernheim, 2008; Tusche et al., 2010), provides a biological foundation for understanding the judgments and decisions that underlay choices, and, more broadly, may shed light on why individuals make the choices that they do (Plassmann, Ambler, and Braeutigam, 2007). Further, neural data has proven useful (albeit, differentially) in choice prediction and forecasting both at the individual (Knutson et al., 2007) and aggregate levels (e.g., Tong et al., 2020).

In the past, traditional economic (e.g., revealed preferences) and psychological theories (e.g., behaviorism) have consistently shown that past choices are the best indicator of future choices (Bernheim, 2008). Initial neuroimaging evidence suggests that neural activity data can complement past choice data and may provide unique insights into forecasts of future choices.

So called, 'neuroforecasting' is the use of brain activity from a sample group of individuals to forecast aggregate choices or preferences of a separate, independent group of individuals (Knutson & Genevsky, 2018). That said, neuroimaging data can be used to 1) predict individual choices, or 2) forecast aggregate choices. For definitional clarity, 'predict' will subsequently refer to individual-level choices, whereas 'forecast' will subsequently refer at the aggregate-level. One of the key hopes and promises of neuroforecasting is that it will be able to reveal information about consumer preferences that cannot be obtained using conventional market research techniques (e.g., conjoint analysis). Such 'hidden information' may reveal individual's true preferences, particularly in situations when individuals are constrained or cannot/do not want to reveal their true preferences. Additionally, such information revealed through neuroimaging may hold value for scaling to the aggregate. However, at this time, theory underlying how and when neuroforecasting works is in its infancy, and researchers are in the process of attempting to discover its usefulness under different contexts and conditions.

Past research on the neural circuits underpinning anticipated gains and losses serves as a foundation for understanding decision-making and choice (Bechara et al., 1996; Bechara et al., 1999; Kuhnen and Knutson, 2005). More specifically, Knutson et al. (2001) suggest that nucleus accumbens (NAcc) activation correlates with individual gain prediction, while ventromedial prefrontal cortex (vmPFC) activation correlates with gain prediction error. This is evidenced by the NAcc having been correlated with self-reported positive arousal, and the anticipation and outcome of potential financial gains being correlated with activity in the NAcc and vmPFC, respectively (Knutson et al., 2001). Anticipated losses, on the other hand, are believed to be driven by insula activity (Paulus and Stein, 2006). This is evidenced by insula activity having been correlated with self-reported negative arousal and observed in anticipation of physical pain

(Büchel and Dolan, 2000; Paulus et al., 2003). In the context of purchase decisions, Knutson et al. (2007) show that NAcc activity correlates with product preference (i.e., anticipated gain prediction), while excessive price correlates with insula activity and deactivation in the vmPFC (i.e., gain prediction error/anticipated loss). While such research provides a foundation for understanding the neural foundations of individual choice, research on neuroforecasting of aggregate choice is scant. In particular, it is unclear how useful neural regions associated with individual choice are for aggregate choice prediction.

At present, a small number of studies have provided a proof of concept for neuroforecasting aggregate choice. In these experiments, a small group of participants (n = ~20-40) are shown unfamiliar, novel, (often) real-world stimuli, and their neural activity data is used to forecast the real-world outcomes of the stimuli once the market has matured (several months or years later). Such neuroforecasts have been reported for music album sales (Berns & Moore, 2012), call-back rates (Falk, Berkman, and Lieberman, 2012), various ad metrics (Venkatraman et al., 2015; Kühn, Strelow, and Gallinat, 2016), health communications (Falk et al., 2016), loan/funding appeals (Genevsky and Knutson, 2015; Genevsky, Yoon, and Knutson, 2017), and online attention markets such as Youtube.com (Tong et al., 2020). In nearly all of these studies, the NAcc and vmPFC (separately or together) contributed to aggregate choice prediction. However, exactly how these two brain areas contribute to aggregate choice prediction, their prediction weights, or the conditions in which each/either is effective, is not yet clear.

Knutson and Genevsky (2018) propose that the affective-integration-motivation framework could provide a theoretical foundation for understanding the differences between neural mechanisms (and regions) most useful for predicting individual choices, and, importantly, how these choices may scale to aggregate choice forecasting. The goal of the present research is

to advance our understanding of decision-making and choice by attempting to forecast aggregate choices in an online dating context using neural activity data (i.e., neuroforecasting). In accordance with the affective-integration-motivation framework, we investigate the notion that affective neural components of individual choice may be most useful for aggregate forecasting, whereas informational/integrative neural components of individual choice will play an additional key role in understanding and predicting individual-level choices. Additionally, by mapping behavioral measures to AIM framework components, we attempt to illustrate the usefulness of neuroimaging data relative to behavioral measures within the context of AIM, choice prediction, and forecasting.

At first glance, and given past neuroimaging research on individual choice, neuroforecasting aggregate choice may seem relatively elementary; to forecast at the aggregate level, simply scale the neural components that have proven fruitful for individual-level choice prediction. However, it is not as simple to forecast aggregate choices in the future/out of sample as it may seem. Rather, it is not yet clear how individual-level choice prediction indicators scale to the aggregate when forecasting choices. Previous theorizing has given rise to a spectrum of theory on scaling to the aggregate. On one end of the spectrum, the no-scaling account proposes that individual-level choice data do not provide any useful information about aggregate market outcomes (Fama, 1970). On the other end of the spectrum, the total-scaling account proposes that given the right model of individual choice, one can simply scale this model to obtain accurate aggregate-level choice forecasts (Von Neumann & Morgenstern, 1944). Finally, partial scaling assumes that some aspects of individual choice may generalize to aggregate, market-level choice better than others. Based on the relatively small sample of research examples, neuroforecasting

of aggregate choice seems to be in accordance with a partial scaling account of forecasting aggregate choice (Knutson and Genevsky, 2018).

Under partial scaling, Knutson & Genevsky (2018) propose that the affect-integration-motivation (AIM) model (Samanez-Larkin & Knutson, 2014) could provide a useful framework for understanding which brain regions may forecast aggregate choice. Specifically, affective components of individual choice, captured by brain activity in the ventral striatum (namely, the NAcc) may be most useful for aggregate forecasting, whereas neural regions associated with integrating affective (and other) information into one's individual goals and context, captured by brain activity in the vmPFC, may prove useful for prediction of individual choices (in addition to affective information). That said, disentangling the contribution of affective and informational components of stimuli, as applied to the decision-making process, requires that researchers have choice decomposition information at both the sample and market level. One of the key appeals of previous neuroforecasting studies has been their use of real-world market-level outcomes serving as a basis for prediction/ forecasting analyses, which makes them highly externally valid. However, given the use of real-world market level stimuli, obtaining individual level information deconstructing choices (i.e., choice decomposition variables), particularly at the market level (indeed, even at the sample level), has not been feasible. For example, researchers may observe whether a crowdfunding campaign was funded (which is based on an aggregation of individual donation choices) and use this variable as the aggregate market-level outcome to be forecast, but the crowdfunding outcome may be the only observed data point at the market level. Stated differently, in such a study the researchers likely do not observe the preferences of users who viewed the crowdfunding profiles and therefore cannot decompose the contribution of various stimuli components on choices, or how such preferences/choices scale to the aggregate outcome.

Such choice decomposition variables are necessary for disentangling the contribution of behavioral variables and neural areas (and their interaction) to overall choice prediction/ forecasting and are unobserved in previous neuroforecasting studies. For these reasons, in this research we have created a simulated market-level dataset, where both market-level choices and choice decomposition variables are observed in the context of online dating.

Online dating profiles provide a suitable and interesting context for our research question for the following reasons: 1) online dating profiles consist of components that are both affective (primarily, a facial image) and informational (e.g., age, location, profile description), 2) mate selection/ preference is a fundamental, evolutionarily relevant behavior, and 3) online dating is a novel market for neuroforecasting.

To test whether the AIM model is suitable for explaining the partial scaling account of neuroforecasting aggregate choice, in this study we have attempted to forecast the success of online dating profiles using independently sampled behavioral and neuroimaging data, and were guided by the following hypotheses:

> H1: Affective neural components, captured by activity in the NAcc, will be most highly correlated with perceived attractiveness and personality, and generalize more broadly across individuals than vmPFC activity, thus proving useful in forecasting aggregate out of sample choices.

> H2: Neural activity associated with integration, captured by activity in the vmPFC, will be most highly correlated with perceptions of career prospects and perceptions of being liked back by the individual in the profile, and, by

incorporating more individual-specific multidimensional considerations, will add value for predicting choices within sample and at the individual-level.

Methods

Dating Profile Stimuli Generation

Using faces from the Chicago Face Database (CFD; Ma, Correll, & Wittenbrink, 2015), we created 36 standardized dating profiles (see Figure 2.1 for example profiles). Profiles were orthogonalized using a 3 x 2 x 2 x 3 factorial design with the following factors and levels: attractiveness (high, medium, low), age (19-23, 24-28), facial expression (neutral, smiling), and profile description (hobbies/likes, socioeconomic status/occupation, and personality traits).

To create standardized dating profiles, we first retained only Caucasian female faces that had both neutral and smiling facial images available in the CFD. The CFD contains metadata for all facial images; these data include summary information on perceptions of the facial images, as rated by an independent sample, with data ranging from average ratings of attractiveness to ratings of facial expressions (e.g., degree of sadness, anger, happiness, etc.). Selected facial images were restricted to those whose perceived age was between 18 and 28, and the CFD attractiveness ratings metadata was used to split faces by attractiveness for the factorial design. Additionally, attractiveness was controlled for between facial expression factor levels; mean attractiveness of the selected neutral ($M = 4.3$, $SD = 0.15$) and smiling ($M = 4.0$, $SD = 0.41$) faces did not differ significantly ($t(34) = 1.61$, $p = .11$). Perceived age of the individual across attractiveness factor levels was also controlled for; mean perceived age among the high attractiveness ($M = 24.42$, $SD = 6.87$), medium attractiveness ($M = 24.81$, $SD = 1.88$), and low attractiveness ($M = 25.25$, $SD = 1.19$) faces did not differ significantly ($F(2, 33) = 0.57$, $p = 0.57$). Names on profiles were randomly selected, without replacement, from a list of the top 54

names from the birth year 1995 created using the 'Popular Names by Birth Year' feature on the USA Social Security website (Popular Baby Names, 2020). Age displayed on each profile was randomly determined within the high (24-28) and low (19-23) age ranges, based on the factorial design (e.g., if a profile is in the younger age category based on the factorial design, a number between 19 and 23 was randomly assigned to the profile). Location displayed on the profile (miles away from participant) was randomly determined between 1 and 50 miles. Profile description factor levels consisted of a list of 3 pieces of information drawn from different sources (based on the desired manipulation). For the hobbies/ likes factor level, which acts as the control profile description condition, the goal was to represent the idiosyncratic likes, interests, and hobbies often found in dating profile descriptions, which should not influence profile perceptions in any systematic way. These hobbies/ likes descriptions were created by randomly combining information from internet lists of the most popular musicians/ artists (e.g., Ariana Grande, Post Malone, Queen), foods (e.g., nachos, peanut butter, steak), and activities (e.g., talking to friends, basketball, picnics, etc.). For the socioeconomic status/occupation factor level, we combined two hobbies/ likes from the same lists as the hobbies/ likes profile description condition with a piece of information about the individual's career path or prospects (e.g., Aspiring surgeon, Law student, Econ Major). Lists of high socioeconomic status/ high earning potential careers were generated from combined information from Georgetown University's Economic Value of College Majors report (Carnevale, Cheah, & Hanson, 2015) and the U.S. Bureau of Labor Statistics list of highest paying occupations (Highest Paying Occupations, 2020). For the personality factor level, we selected words from Chandler's (2018) list of person descriptive words shown to increase likableness (e.g., honest, kind). To reduce demand artifacts resulting from participants making clear distinctions between profile description factor levels,

personality factor level profiles were randomly determined to display two or three personality words – in the case when two personality words were displayed, a hobby/ like word was randomly included to maintain consistency of three pieces of information displayed in all profile descriptions, regardless of factor level. Two additional profiles were created as attention checks, using faces that were not part of the main profile set, with information on how participants should respond presented in the description area (e.g., 'like this profile'). All profiles were generated in R.

Task

In all versions of the task, participants were instructed that they would "make judgments about online dating profiles" and were given the opportunity to view two supplementary profiles (not included as part of the main trials) to become comfortable with the protocol. During the task, participants were shown all 36 profiles and 2 attention checks (within-subjects), in random order, and made a binary 'like' or 'pass' choice for each profile, followed by rating each profile on four choice decomposition items using a 7-point Likert scale (note: for all analyses, choice decomposition variable data were ipsatized). For each profile, participants made a binary 'like' or 'pass' choice while viewing the profile. The profile then disappeared, and participants completed the four choice decomposition items, which read: "This individual…" 1) "is physically attractive", 2) "has good career prospects", 3) "has a likable personality", and 4) "is likely to like me back and respond to my messages". After completing the binary like/pass portion of the task, participants also completed a supplementary rank order task, in which they were asked to rank order their preferences for seven randomly selected profiles. For brevity, analyses from the rank order task are not presented or discussed in this chapter. Lastly, participants completed two 7-point Likert items on perceptions of their own attractiveness: "I am

physically attractive" and "Other people find me physically attractive", which were averaged to create a self-rated attractiveness variable.

Participants completed informed consent prior to the task, were debriefed following the task, and all procedures were approved by the University of Michigan's Health Sciences and Behavioral Sciences institutional review board and the Temple University Ethics and Compliance Office.

Samples

Participant samples consisted of heterosexual cisgender Caucasian males between the ages of 18 and 35 who were not in a committed relationship at the time of the task. Although racial effects in mate preferences are interesting in their own right, previous research has consistently documented racial homophily (i.e., strong same race preferences) in human sexual/romantic relationships (McClintock et al., 2010; Fisman et al., 2008). Further, the Chicago Face Database has more facial expression images available for Caucasians and African-Americans than other races. Given that the present research question does not involve racial effects of mate preference, and previous research has shown that race can dramatically influence mate preferences, we chose to restrict the participant sample and profiles to the most readily accessible race and sexual orientation in the populations that we would be recruiting from.

In-lab (Behavioral) Sample. For independent behavioral modeling, an in-lab sample (N = 45; M = 20.18, SD = 1.35) was collected at the University of Michigan, Ann Arbor, and Temple University using the fMRI scanner-ready E-Prime 3.0 (Psychology Software Tools, Inc., 2020) version of the task.

fMRI Sample. The neuroimaging sample consisted of 29 healthy right-handed participants (M= 26.41, SD = 4.35), who completed a scanner-compatible version of the task in

E-Prime 3.0 at the Temple University Brain Research & Imaging Center (TUBRIC). During the scanner version of the task, profiles were presented as follows: a 2, 4, or 6 second presentation of a fixation cross jitter (randomly selected for each trial), followed by a 2 second viewing of the left side of the profile only (which shows the facial image), followed by 4 seconds of viewing the entire profile (including the facial image and profile description). After this 6 second trial/ viewing period, 'Like' and 'Pass' options appeared on the screen and participants had 4 seconds to make a response. The 'Like' and 'Pass' buttons appeared in green and red boxes, respectively, and left/ right orientation was randomized between trials. Upon making a selection, participants immediately received confirmation of their selection (e.g., 'Like') via a 1 second feedback screen, and any additional time between the response and timed response period (4 seconds) was added to the intertrial interval jitter fixation period (see Figure 2.2 for a visual representation of the fMRI scanner trial time course). To reduce participant time in the scanner, only binary like/ pass judgements were conducted in the scanner. Participants in the fMRI sample completed profile judgements of the four choice decomposition variables and the ranking task in a behavioral lab space immediately following the neuroimaging session (outside of the scanner).

Simulated Market-level Sample. Market-level data was collected using a Qualtrics version of the task via two online participant panels (ROI Rocket and Cint; $N = 654$; $M = 26.62$, $SD = 5.22$). Given online data collection quality concerns, only data from participant who passed all attention checks was included in the analysis. To determine the sample size necessary to adequately power the simulated market-level dataset, we ran a 41-participant pilot test and used data from the pilot to conduct a-priori power calculations, which suggested that a sample size of greater than 385 was necessary to achieve statistical power greater than 99% for the task. Post-

hoc power analysis of the market-level sample revealed that a power >97% within the market level sample was achieved.

A principal components analysis was performed on the four choice decomposition variables (attractiveness, career prospects, likeable personality, and likelihood of likeback) confirming that each choice decomposition variable was capturing unique information about the stimuli (>10% unique variance per item).

Classification Analysis

For classification analysis, data were randomly divided into training (70%) and testing (30%) sets, at the profile level. All classification analysis was conducted using the caret package in R (Kuhn, 2008) using logistic regression models for individual choice and ordinary least squares (OLS) regression at the aggregate level of analysis. Model selection and parameter optimization were conducted using the in-lab sample and fMRI sample training sets (i.e., models were not trained using any simulated market level data, since these data would not be observed to a marketer in a real-world setting), using 10-fold cross-validation. Model accuracy was tested on the remaining 30% of independent test set profiles, such that model accuracy always represents prediction/forecasts on profiles unobserved in the training set. All prediction/forecasting accuracy results represent the average of 50 iterations for each classification analysis.

At the individual level, prediction accuracy represents the percentage of correct like versus pass binary choices. Therefore, chance prediction at the individual level is 50% for the binary choice task. At the aggregate level, outcome variables are the averaged across participants at the profile level, and thus forecasting accuracy represents the percentage of forecasts that estimate the choice likelihood (the probability that a given profile will be liked) for a profile

within a +/- 5% interval, as choice likelihood varies continuously from 0 (nobody 'likes the profile) to 1 (all participants 'like' the profile). Therefore, chance forecasting accuracy at the aggregate level for the binary choice task is 10%.

fMRI Acquisition and Data Analysis

Neuroimaging data was acquired using a Siemens Magnetom Prisma 3T MRI system with a 64-channel head coil at the Temple University Brain Research & Imaging Center (TUBRIC). First, we acquired high resolution whole-brain T1-weighted anatomical scans (repetition time (TR): 2400ms; echo time (TE): 2.28ms; inversion time (TI): 1150ms; acquisition matrix: 256 x 256; flip angle: 8 degrees). During the task, functional images were acquired using a T2*-weighted gradient-echo echo-planar imaging (EPI) sequence sensitive to blood-oxygenation-level dependent (BOLD) contrast. Functional volumes contained 36 slices parallel to the axial plane connecting the anterior and posterior commissures (TR: 2080ms; TE: 28ms; matrix: 68 x 68; flip angle: 80 degrees). To make responses during the task, participants used their right hand to press buttons on a five-button Celeritas Button Response Unit (Psychology Software Tools, Inc., 2020). Imaging data were organized in accordance with the brain imaging data structure (BIDS) standard (Gorgolewski, 2016). Neuroimaging quality control checks were conducted via MRIQC (Esteban et al., 2017) and primary imaging analysis was conducted using Statistical Parametric Mapping in MATLAB (SPM, 2021; MathWorks, 2021).

Preprocessing Pipeline. Neuroimaging analyses in this chapter come from preprocessing performed using FMRIPREP (Esteban et al., 2020), a Nipype (Gorgolewski et al., 2011) based tool. Each T1w (T1-weighted) volume was corrected for INU (intensity non-uniformity) using N4BiasFieldCorrection v2.1.0 (Tustison et al., 2010) and skull-stripped using antsBrainExtraction.sh v2.1.0 (using the OASIS template). Spatial normalization to the ICBM

152 Nonlinear Asymmetrical template version 2009c (Fonov et al., 2009) was performed through nonlinear registration with the antsRegistration tool of ANTs v2.1.0 (Jenkinson et al., 2002) using brain-extracted versions of both T1w volume and template. Brain tissue segmentation of cerebrospinal fluid (CSF), white-matter (WM) and gray-matter (GM) was performed on the brain-extracted T1w using fast (Zhang, Brady, & Smith, 2001; Jenkinson et al., 2012; FSL v5.0.9).

Functional data were slice time corrected using 3dTshift from AFNI v16.2.07 (Cox, 1996) and motion corrected using mcflirt (FSL v5.0.9). This was followed by co-registration to the corresponding T1w using boundary-based registration (Greve & Fischl, 2009) with six degrees of freedom, using flirt (FSL). Motion correcting transformations, BOLD-to-T1w transformation and T1w-to-template (MNI) warp were concatenated and applied in a single step using antsApplyTransforms (ANTs v2.1.0) using Lanczos interpolation.

Physiological noise regressors were extracted applying CompCor (Behzadi et al., 2007). Principal components were estimated for the two CompCor variants: temporal (tCompCor) and anatomical (aCompCor). A mask to exclude signal with cortical origin was obtained by eroding the brain mask, ensuring it only contained subcortical structures. Six tCompCor components were then calculated including only the top 5% variable voxels within that subcortical mask. For aCompCor, six components were calculated within the intersection of the subcortical mask and the union of CSF and WM masks calculated in T1w space, after their projection to the native space of each functional run. Frame-wise displacement (Power et al., 2013) was calculated for each functional run using the implementation of Nipype.

Many internal operations of FMRIPREP use Nilearn (Abraham et al., 2014), principally within the BOLD-processing workflow. Finally, imaging data was smoothed in SPM using a 4mm smoothing kernel.

Region of Interest Extraction. Blood-oxygen-level-dependent signal (Ogawa et al., 1990) was extracted from regions of interest (ROIs) using the REX (NITRC: REX, 2021) and MarsBaR (Brett et al., 2002) SPM toolboxes for regionally targeted analysis in the NAcc and vmPFC. Within MATLAB, raw BOLD activity was extracted from functional images using REX with weighted means, scaled within each ROI. For BOLD activity extracted using MarsBaR, data were extracted from first level individual stimuli SPM contrasts, generated from models that included a regressor for each trial (4s duration), hand motion, 8 standard motion regressors ("trans_x", "trans_y", "trans_z", "rot_x", "rot_y", "rot_z", "csf", "white_matter"), and scaling the grand mean to 0. Additionally, for BOLD extraction in the vmPFC, 2s was added to trial onset times since the first 2s in the trial presentation sequence consisted of only face viewing. Montreal Neurological Institute (MNI) coordinates for ROI were converted from Talairach coordinates in Genevsky, Yoon, and Knutson (2017) using BioImage Suite (Yale BioImage Suite, 2020): NAcc [-10, 14, -6] (left) and [11, 15, -6] (right) and vmPFC [-4, 50, 1] (left) and [5, 50, 1] (right).

Results

Market-level Descriptive Statistics and Modeling

To validate that elements of the factorial design were influencing participants' judgements and decisions about profiles as expected, we first present individual level trends from the fully powered market sample. Table 2.1 shows regression results for binary choice, and each choice decomposition variable, using only factorial elements as predictors. Overall, factorial elements were highly predictive of both choice and all choice decomposition variables, with

estimates directionally consistent with expectations based on the factorial design: factorial attractiveness bins should increase ratings of attractiveness, smiling facial images should increase personality and like back ratings, SES/ occupation indicators should increase ratings of career prospects, etc. Factorial design attractiveness levels were consistent with participants' attractiveness ratings of profiles, with the highest attractiveness bin factorial element having the highest ratings of attractiveness (M = 5.09, SD = 1.46), followed by profiles in the medium attractiveness bin (M = 4.31, SD = 1.65) and low attractiveness bin (M = 3.88, SD = 1.62; F(2, 23541) = 1172, $p < 0.001$). Factorial design based SES/occupation indicators in a profile description led to participants rating the profiles as having better career prospects (M = 5.30, SD = 1.48), than profiles with positive personality indicators in the profile description (M = 4.41, SD = 1.27), or control profiles with hobbies listed in the profiles description (M = 4.20, SD = 1.24, F(2, 23541) = 1506, $p < 0.001$). Participants rated profiles with a smiling face higher on positive personality characteristics (M = 4.73, SD = 1.43) than profiles with a neutral face (M = 4.52, SD =1.43; t(23542) = -11.49, $p < 0.001$) and participants rated profiles with a smiling face as more likely that the individual in the profile will be more willing to 'like' them back (M = 4.31, SD = 1.46) than profiles with a neutral face (M = 4.08, SD = 1.45; t(23542) = -12.01, $p < 0.001$). Figure 2.3 illustrates key trends in the market data.

Additionally, since a primary goal of this research was to break down choice prediction using choice decomposition variables, a series of robustness checks were run to ensure that each of the choice decomposition variables uniquely contributes to choice. Table 2.2 contains logistic regressions with binary choice regressed on choice decomposition variables and factorial elements. Within the simulated market sample, estimates for choice decomposition variables are robust across models that include or exclude: 1) factorial design elements, 2) participant-level

age and self-rated attractiveness control variables, and 3) participant and profile level random effects. Importantly, all of the choice decomposition variables had a significant positive contribution on binary choice in the fully powered simulated market level sample, with attractiveness having the largest effect (attractiveness: $z = 51.62$, $p < 0.001$; career: $z = 9.68$, $p < 0.001$, personality: $z = 25.92$, $p < 0.001$, likeback: $z = 19.55$, $p < 0.001$).

Predicting Individual Choice

Behavioral Correlates of Individual Online Dating Choices. Participants liked profiles an average of 12.58 times in the lab sample (*SD* = 7.40; range = 1–35), 14.76 times in the fMRI sample (*SD* = 5.93; range = 1–26), and 17.49 times in the simulated market data (*SD* = 8.68; Range = 0–36), out of 36 profiles.

Within the in-lab sample, individual binary like versus pass choices were correlated with ratings of attractiveness ($r = 0.61$, $t(1618) = 31.26$, 95% *CI* [0.58, 0.64], $p < 0.001$), career prospects ($r = 0.19$, $t(1618) = 7.87$, 95% *CI* [0.15, 0.24], $p < 0.001$), personality ($r = 0.37$, $t(1618) = 16.18$, 95% *CI* [0.33, 0.41], $p < 0.001$), and likeback ($r = 0.26$, $t(1618) = 10.84$, 95% *CI* [0.21, 0.31], $p < 0.001$) choice decomposition variables. Within the fMRI sample, individual binary like versus pass choices were correlated with individual ratings of attractiveness ($r = 0.48$, $t(1039) = 17.81$, 95% *CI* [0.44, 0.53], $p < 0.001$), personality ($r = 0.38$, $t(1039) = 13.10$, 95% *CI* [0.32, 0.43], $p < 0.001$), and likeback ($r = 0.16$, $t(1039) = 5.26$, 95% *CI* [0.10, 0.22], $p < 0.001$), but not career prospects ($r = 0.02$, $t(1039) = 0.81$, 95% *CI* [-0.04, 0.09], $p = 0.42$). Finally, within the simulated market sample, individual binary like versus pass choices were correlated with all choice decomposition variables (attractiveness: $r = 0.54$, $t(23542) = 98.96$, 95% *CI* [0.53, 0.55], $p < 0.001$; career prospects: $r = 0.19$, $t(23542) = 30.49$, 95% *CI* [0.18, 0.21], $p < 0.001$; personality ratings: $r = 0.40$, $t(23542) = 66.39$, 95% *CI* [0.39, 0.41], $p < 0.001$; likeback: $r =$

0.29, $t(23542) = 46.78$, 95% *CI* [0.28, 0.30], $p < 0.001$). Correlation coefficients between choice decomposition variables and profile factorial elements can be found in Table 2.3 for in-lab sample data, Table 2.4 for fMRI sample data, and Table 2.5 for simulated market data.

Neural Correlates of Individual Online Dating Choices. In the fMRI sample, individual NAcc activity was significantly correlated with binary choice ($r = 0.16$, $t(1039) = 5.12$, 95% *CI* [0.10, 0.22], $p < 0.001$), and choice decomposition variables attractiveness ($r = 0.15$, $t(1039) = 4.92$, 95% *CI* [0.09, 0.21], $p < 0.001$), personality ($r = 0.09$, $t(1039) = 2.84$, 95% *CI* [0.03, 0.15], $p < 0.01$), and likeback ($r = 0.10$, $t(1039) = 3.28$, 95% *CI* [0.04, 0.16], $p < 0.01$), but not with ratings of career prospects ($r = -0.02$, $t(1039) = -0.65$, 95% *CI* [-0.08, 0.04], $p = 0.52$). Conversely, individual vmPFC activity was only correlated with binary choice ($r = 0.13$, $t(1039) = 4.13$, 95% *CI* [0.07, 0.19], $p < 0.001$) and likeback ($r = 0.11$, $t(1039) = 3.44$, 95% *CI* [0.05, 0.17], $p < 0.001$) among choice decomposition variables, but not correlated with choice decomposition variables attractiveness ($r = 0.04$, $t(1039) = 1.18$, 95% *CI* [-0.02, 0.10], $p = 0.24$), career prospects ($r = 0.02$, $t(1039) = 0.51$, 95% *CI* [-0.04, 0.08], $p = 0.61$), or personality ($r = 0.06$, $t(1039) = 1.81$, 95% *CI* [0.00, 0.12], $p = 0.07$). Activity in the NAcc and vmPFC was significantly correlated during the task ($r = 0.42$, $t(1039) = 14.92$, 95% *CI* [0.37, 0.47], $p < 0.001$). Correlation coefficients between NAcc and vmPFC, choice decomposition variables, and profile factorial elements can be found in Table 2.4.

Regression Analyses of Individual Dating Profile Decisions. To understand the contribution of individual choice breakdown variables to choice, we ran logistic regressions using in-lab sample level, fMRI sample level, and simulated market-level individual choices regressed on choice decomposition variables, factorial elements, and neural ROI data (separately and together). Within the in-lab sample, among choice decomposition variables, individual

ratings of attractiveness ($z = 16.66$, $p < 0.001$), personality ($z = 5.74$, $p < 0.001$), and likeback ($z = 7.59$, $p < 0.001$) choice decomposition variables were significantly associated with binary choice (see Model 1, Table 2.6), while individual ratings of career prospects were not ($z = 1.92$, $p = 0.06$). In the fMRI sample, among choice decomposition variables, individual ratings of attractiveness ($z = 12.17$, $p < 0.001$) and personality ($z = 7.20$, $p < 0.001$) choice decomposition variables were significantly associated with binary choice, while ratings of career prospects ($z = -1.48$, $p = 0.14$) and likeback were not ($z = 1.84$, $p = 0.07$; see Model 1, Table 2.7). Additionally, a regression model including only brain activity data (see Model 3, Table 2.7) illustrates that NAcc activity was significantly associated with individual binary choice ($z = 3.96$, $p < 0.001$), while vmPFC activity was not ($z = 1.53$, $p = 0.13$). The association between NAcc activity and binary choice was partially attenuated when brain activity data was combined in a regression with profile factorial information (Model 5, Table 2.7; $z = 3.11$, $p < 0.01$), and fully eliminated when brain activity data was combined in a regression with choice decomposition variable ratings (Model 4, Table 2.7; $z = 1.69$, $p = 0.09$) as well as in a model with both choice decomposition variable ratings and profile factorial information (Model 6, Table 2.7; $z = 1.61$, $p = 0.11$). Multiple partial F-test comparisons revealed that neural activity data in the NAcc and vmPFC significantly contributed to choice model fit over and above nested models with choice decomposition variables ($\chi^2(2) = 8.27$, $p < 0.05$) and factorial elements ($\chi^2(2) = 22.28$, $p < 0.001$).

As likeback serves as the primary behavioral measure of the integrative phase of AIM, we additionally conducted similar regression analyses using individual likeback ratings as the dependent variable in the fMRI sample. Crucially, while only personality ($t = 10.03$, $p < 0.001$) was associated with likeback ratings among choice decomposition variables (see Model 1, Table

2.8), NAcc activity ($t = 2.02$, $p = 0.04$) and vmPFC activity ($t = 2.28$, $p = 0.03$; see Model 3, Table 2.8) were significantly associated with individual likeback ratings. Additionally, as choice decomposition variables or factorial elements were added to models with brain data, the association between NAcc and likeback ratings was eliminated ($t = 1.42$, $p = 0.16$; $t = 1.93$, $p = 0.05$) while the association between vmPFC and likeback ratings was not ($t = 2.14$, $p = 0.03$; $t = 2.34$, $p = 0.02$; see Models 4 and 5, Table 2.8).

Whole Brain and ROI Predictors of Individual Dating Profile Liking. Whole-brain analyses in SPM contrasted brain activity (BOLD signal) during dating profile presentation (i.e., initial 6s after stimuli onset) in trials in which participants liked profiles versus trials in which participants passed on profiles. Averaged group brain activity (n = 29) revealed a single significant cluster of brain activity at SPM coordinates [-6, 38, -7], which was predictive of individual liking but not consistent with NAcc or vmPFC ROIs. However, investigating brain activity within pre-specified regions of interest (ROI) revealed that NAcc ($t(27) = 3.44$, 95% CI [0.06, 0.25], $p < 0.01$) and vmPFC ($t(27) = 4.74$, 95% CI [0.24, 0.61], $p < 0.001$) activity were greater during presentations of liked versus passed dating profiles (in-text t-statistics calculated according to spherical ROI analysis protocol in Andy's Brain Book, 2019; see Figure 2.4 and 2.5). Figures 2.6 and 2.7 show the brain activity time course plots for the NAcc and vmPFC ROIs, respectively. As expected under the AIM framework, significant increases in BOLD activity for liked profiles occurred earlier for NAcc (~TRs 3-4, with maximum differential between liked and passed BOLD activity occurring at TR 3) than for vmPFC (~TRs 3-7, with maximum differential between liked and passed BOLD activity occurring at TR 4).

Classification of Individual Dating Profile Liking. In-lab and fMRI sample choice decomposition variables were used to train logistic regression models to predict individual-level

binary choices. At the individual-level of prediction, within the in-lab sample the model trained with all choice decomposition variables together resulted in the highest binary choice prediction accuracy in the hold out data, at 75% accuracy (see Table 2.9), followed by models with trained using attractiveness ratings (73% accuracy) and only personality ratings (61% accuracy), while models trained exclusively on career prospects ratings (52% accuracy) and likeback ratings (55% accuracy) predicted binary choice at levels close to chance. In the fMRI sample, the highest prediction accuracy within-sample came from models trained using all choice decomposition variables (77% accuracy) and combining all choice decomposition variables with neural activity in the vmPFC (78% accuracy). While adding NAcc activity along with choice decomposition variables as a classifier (76% accuracy) did not increase prediction accuracy over and above a model with choice decomposition variables on their own (77% accuracy), adding vmPFC activity did increase prediction accuracy (78% accuracy). In models trained using fMRI sample choice decomposition variables, but tested on out-of-sample hold out simulated market choices, the models that were trained using all choice decomposition variables again performed the best (76%), followed by models trained individually with attractiveness (75%) and personality (66%), while models using career prospects (51%) and likeback (57%) performed marginally better than chance (see Table 2.10).

Forecasting Aggregate Choice

Behavioral Correlates of Aggregate Online Dating Choices. Overall average aggregate choice likelihood rates were 35.94% in the in-lab sample (*SD* = 22.54%; Range = 2.22–86.67%), 41.10% in the fMRI sample (*SD* = 22.40%; Range = 6.90-86.20%), and 45.60% in the simulated market data (*SD* = 18.30%; Range = 13.60-86.54%).

Within the in-lab sample, aggregate choice likelihood was correlated with aggregate ratings of attractiveness ($r = 0.96$, $t(34) = 19.68$, 95% *CI* [0.92, 0.98], $p < 0.001$) and personality ($r = 0.73$, $t(34) = 6.31$, 95% *CI* [0.53, 0.86], $p < 0.001$) among choice decomposition variables, but not aggregate ratings of career prospects ($r = 0.29$, $t(34) = 1.79$, 95% *CI* [-0.04, 0.57], $p = 0.08$) or likeback ($r = 0.30$, $t(34) = 1.84$, 95% *CI* [-0.03, 0.57], $p = 0.07$). Similarly, within the fMRI sample aggregate choice likelihood was significantly correlated with aggregate ratings of attractiveness ($r = 0.90$, $t(34) = 12.07$, 95% *CI* [0.81, 0.95], $p < 0.001$) and personality ($r = 0.60$, $t(34) = 4.34$, 95% *CI* [0.33, 0.77], $p < 0.001$) among choice decomposition variables, but not aggregate ratings of career prospects ($r = -0.08$, $t(34) = -0.49$, 95% *CI* [-0.40, 0.25], $p = 0.63$) or likeback ($r = 0.17$, $t(34) = 1.02$, 95% *CI* [-0.17, 0.47], $p = 0.31$). Finally, within the simulated market sample, aggregate choice likelihood was significantly correlated with aggregate ratings of attractiveness ($r = 0.97$, $t(34) = 23.86$, 95% *CI* [0.94, 0.99], $p < 0.001$), personality ($r = 0.81$, $t(34) = 8.17$, 95% *CI* [0.66, 0.90], $p < 0.001$), and likeback ($r = 0.56$, $t(34) = 3.96$, 95% *CI* [0.29, 0.75], $p < 0.001$) among choice decomposition variables, but not career prospects ($r = 0.13$, $t(34) = 0.79$, 95% *CI* [-0.20, 0.44], $p = 0.44$). Correlation coefficients between aggregate ratings of choice decomposition variables and profile factorial elements can be found in Table 2.11 for in-lab sample data, Table 2.12 for fMRI sample data, and Table 2.13 for simulated market data.

Neural Correlates of Aggregate Online Dating Choices. In the fMRI sample, aggregate NAcc activity was significantly correlated with aggregate choice likelihood ($r = 0.76$, $t(34) = 6.82$, 95% *CI* [0.57, 0.87], $p < 0.001$), and choice decomposition variables attractiveness ($r = 0.67$, $t(34) = 5.30$, 95% *CI* [0.44, 0.82], $p < 0.001$) and personality ($r = 0.36$, $t(34) = 2.28$, 95% *CI* [0.04, 0.62], $p < 0.05$). Conversely, aggregate vmPFC activity was not significantly correlated with aggregate binary choices ($r = 0.04$, $t(34) = 0.25$, 95% *CI* [-0.29, 0.37], $p = 0.80$)

and was only significantly correlated with aggregate ratings of the likeback among choice decomposition variable ($r = 0.38$, $t(34) = 2.36$, 95% *CI* [0.05, 0.63], $p < 0.05$).

Using fMRI sample aggregate means, NAcc activity was also correlated with simulated market level aggregate binary choice ($r = 0.67$, $t(34) = 5.22$, 95% *CI* [0.43, 0.81], $p < 0.001$) and aggregate attractiveness ($r = 0.68$, $t(34) = 5.48$, 95% *CI* [0.46, 0.83], $p < 0.001$) and personality ($r = 0.47$, $t(34) = 3.07$, 95% *CI* [0.16, 0.69], $p < 0.01$) among choice decomposition variables. Aggregate vmPFC activity in the fMRI sample was not significantly correlated with simulated market level aggregate choice or any choice decomposition variables.

Aggregate activity in the NAcc and vmPFC was not significantly correlated at the profile presentation level during the task ($r = 0.09$, $t(34) = 0.55$, 95% *CI* [-0.24, 0.41], $p = 0.59$). Correlation coefficients between aggregate NAcc and vmPFC activity, choice decomposition variables, and profile factorial elements can be found in Table 2.12.

Regression Analyses of Aggregate Dating Profile Choices. To understand the contribution of aggregate choice breakdown variables on aggregate choice, we ran OLS regressions using aggregate choice likelihood regressed on aggregate choice decomposition variables in the in-lab sample, fMRI sample, and simulated market-level sample. Within the in-lab sample, aggregate attractiveness ($t = 14.78$, $p < 0.001$) and likeback ($t = 3.00$, $p < 0.01$) choice decomposition variables were associated with greater choice likelihood, while aggregate career prospects ($t = 1.83$, $p = 0.07$) and personality ratings ($t = -0.81$, $p = 42$) were not. Using the same in-lab sample aggregate choice decomposition variable means, only aggregate attractiveness was significantly associated ($t = 6.63$, $p < 0.001$) with choice likelihood at the simulated market sample-level (see Table 2.14).

In the fMRI sample, only aggregate attractiveness ($t = 10.47$, $p < 0.001$) was associated with aggregate choice among aggregations of choice decomposition variables and was associated with greater choice likelihood, while aggregate career prospects ($t = -1.22$, $p = 0.23$), personality ratings ($t = 0.64$, $p = 0.52$), and likeback ratings ($t = 2.03$, $p = 0.05$) were not. Aggregate fMRI sample NAcc activity was significantly associated with aggregate choice both within the fMRI sample ($t = 6.72$, $p < 0.001$) and at the simulated market level ($t = 5.14$, $p < 0.001$), while aggregate vmPFC activity was not (fMRI sample: $t = -0.25$, $p = 0.80$; simulated market level: $t = -0.18$, $p = 0.86$; see Table 2.15). Within the fMRI sample, the association between NAcc activity and choice was partially attenuated when aggregate ratings of choice decomposition variables were added to the model ($t = -2.67$, $p < 0.05$), and fully eliminated when aggregate ratings of choice decomposition variables were added to the simulated market level models ($t = 0.48$, $p = 0.63$). Multiple partial F-test comparisons indicated that aggregate neural activity in the NAcc and vmPFC significantly increased forecasting of aggregate choice likelihood within the fMRI sample ($F(2, 29) = 3.58$, $p < 0.05$), but not in the simulated market sample ($F(2, 29) = 0.15$, $p = 0.87$).

Finally, to understand the integrative aspects of AIM, we conducted similar regression analyses using aggregate likeback ratings as the dependent variable in the fMRI sample. Within the fMRI sample, aggregate attractiveness ($t = -2.75$, $p < 0.01$) and aggregate personality ($t = -4.92$, $p < 0.001$) were associated with aggregate likeback ratings, while aggregate career prospects were not ($t = -0.14$, $p = 0.89$). When regressing aggregate simulated market sample likeback ratings on these same choice decomposition variables, only aggregate personality was significantly associated ($t = -5.39$, $p < 0.001$). Crucially, among neural predictors, aggregate vmPFC activity was associated with aggregate likeback ratings within the fMRI sample ($t =$

2.28, $p < 0.05$), but not when forecasting aggregate likeback ratings in the simulated market sample ($t = 0.62$, $p = 0.54$), and aggregate NAcc activity was not associated with aggregate likeback rates within the fMRI sample ($t = 0.56$, $p = 0.58$) or in the simulated market sample ($t = 1.63$, $p = 0.11$; see Table 2.16).

Classification of Aggregate Online Dating Outcomes. Aggregate fMRI sample choice decomposition variables were used to train OLS regression models, uniquely and in combination, to predict aggregate-level choice likelihoods. Training models using aggregate levels of choice decomposition variables (attractiveness, career prospects, personality, and likelihood of 'like' back of profiles) to predict the aggregate choice likelihood of randomly selected holdout profiles (70/30 train/test; 50 iterations) resulted in correct aggregate choice likelihood prediction (+/- 5% of actual choice likelihood) 26.4% of the time in the in-lab sample, 40.2% of the time in the fMRI sample, and 34.0% of the time for the market level choice. In comparison, using only aggregate NAcc from the fMRI sample as a classifier resulted in correct aggregate choice likelihood prediction 17.6% of the time in the in-lab sample, 21.3% of the time in the fMRI sample, and 32.5% of the time for the market level choice.

Within the fMRI sample, the model trained using a combination of all choice decomposition variables produced the best forecasts, at 40.2% accuracy, followed by models trained individually with attractiveness (32%) and personality (18%), while models trained with career prospects ratings (9%) and likeback ratings (7%) performed below chance. Among neuroforecasting models, aggregate NAcc activity predicted aggregate choices within the fMRI sample well above chance at 21% accuracy, while vmPFC activity did not (10%). Using these same classifiers, but forecasting aggregate choices in a hold out from the simulated market sample, the model using aggregate attractiveness produced the highest prediction accuracy at

36%, followed by classifiers with all choice decomposition variables (34%), career prospects (19%), personality (17%), and likeback (13%). Neuroforecasting aggregate choice in the simulated market sample was most effective using only aggregate NAcc activity, at 33% accuracy, while a classifier using only vmPFC activity had an accuracy of 16%. Using both NAcc and vmPFC activity together to forecast aggregate choice results in correct forecasts 28% of the time (see Table 2.17).

Discussion

The promise of neuroscientific data in helping to understand consumer decisions and potential for neural data to aid in forecasting market choices are key topics of exciting novel streams of research in consumer neuroscience, consumer behavior, and marketing. In marketing, brain activity data have revealed profound truths about consumer decision making that otherwise (without fMRI data) would have been largely unattainable, including developments in our understanding of the representation and importance of brand preference (Koenigs and Tranel, 2008), the influential role of expectations, based on price, in evaluations of product quality (Plassmann et al., 2008), and that evaluative judgements of 'brand personalities' are not the same as personality judgements of humans (Yoon et al., 2006). That is, using tools and techniques from the field of neuroscience, consumer neuroscientists have developed and carved out significant insights in the field of marketing. The phenomenon of neuroforecasting, in which the brain activity from a small group of consumers is used to forecast aggregate market level outcomes, stems from a powerful idea previously held to the realm of science fiction. With a number of recent research studies illustrating that neural data can in fact forecast aggregate market choices, a key question remains: how and when does brain beat behavior?

The present research aimed to test the affective-integration-motivation (AIM) framework as a theoretical foundation for understanding how and when brain may in fact beat behavior. The AIM framework posits that while key neural regions in the brains value integration circuit (namely, the vmPFC) can be useful for understanding individual choices, early activity in the affective regions of the brain (namely, the NAcc) may be most powerful for forecasting aggregate choices (Samanez-Larkin and Knutson, 2015). In the context of online dating choices, we created a simulated market-level dataset for forecasting aggregate choices, and forecasted choices by training data from both a small in-lab sample and a sample who completed the task inside of an fMRI scanner. Our design afforded us the opportunity to observe choice decomposition data at all levels of analysis (i.e., asking all participants to rate aspects of profiles that would be considered when making decisions), as well as correlate neural activity with choice decomposition components to understand how different choice decomposition components contributed to prediction and forecasting. In addition to asking participants to make a binary choice (like versus pass) for all online dating profiles, participants were asked to rate all profiles on the following 4 choice decomposition variables: how physically attractive they believe the individual in the profile is (attractiveness), the individuals career potential (career prospects), how likeable they believe that their personality is (personality), and the probability that the individual in the profile will 'like' them back (since most online dating sites require mutual liking for any further interactions; likeback). Overall, the findings from this study are consistent with AIM as a framework for understanding how and when neuroforecasting may be effective, and suggest that researchers and marketers may be able to use neural data to better understand and categorize choice components collected through behavioral/ survey measures. Further, in certain contexts, if behavioral measures can effectively isolate affective and

integrative choice components, marketers may be able to produce excellent forecasting results without the significant investments necessary to obtain neuroimaging data.

Hypothesis Testing. Consistent with the AIM framework, neural activity time courses showed that activity in the NAcc, representing affective evaluation, peaked earlier during the decision processing phase (and before actually indicating a decision) than activity in the vmPFC, which is associated with the value integration phase of AIM (Levy and Glimcher, 2012). Additionally, consistent with H1 the primary affective neural component under investigation, the NAcc, was correlated with choice decomposition variables attractiveness and personality at both the individual and aggregate-levels of analysis. In terms of forecasting using behavioral variables, forecasts made by classifiers trained using only attractiveness produced the highest prediction accuracy among choice decomposition variables (including in comparison to classifiers using all choice decomposition variables together). Finally, while classifiers trained using aggregate vmPFC activity performed relatively poorly at neuroforecasting aggregate market choices (15.8% accuracy), classifiers trained using aggregate NAcc activity did effectively neuroforecast aggregate market choices exceptionally well (32.5% accuracy). Indeed, classifiers trained using both aggregate NAcc and vmPFC activity performed more poorly than classifiers trained using aggregate NAcc activity alone (28.0% accuracy versus 32.5% accuracy).

Partially consistent with H2 the primary integrative neural component under investigation, the vmPFC, was correlated with the likeback choice decomposition variable at both the individual and aggregate-levels, but the career prospects variable was not. In terms of individual choice prediction, classifiers trained using all behavioral choice decomposition variables produced the highest prediction accuracy (versus classifiers trained using each choice decomposition variable separately). Using neural data, neither NAcc activity (58.7% accuracy)

nor vmPFC activity (58.3% accuracy) alone performed particularly well at individual choice prediction. However, in accordance with H2, when introducing neural data to classifiers of binary choice in addition to choice decomposition variables, the highest prediction accuracy resulted from classifiers trained combining choice decomposition variables and vmPFC activity (77.7% accuracy), over classifiers trained combining choice decomposition and NAcc activity (76.5 accuracy), or choice decomposition variables and both NAcc and vmPFC activity (77.5% accuracy).

Forecasting Aggregate Online Dating Outcomes. Consistent with the AIM framework for understanding neuroforecasting, aggregate NAcc activity was highly correlated with aggregate ratings of attractiveness, while aggregate vmPFC activity was most highly correlated with aggregate likeback ratings. Only aggregate NAcc activity was significantly associated with aggregate online dating decision outcomes, both for forecasting within the fMRI sample and in the simulated market sample. Further, when sequentially assessing the impact of choice decomposition variables and neural ROIs on choice, the association between NAcc activity and online dating outcomes was partially attenuated when choice decomposition variables were added to models within the fMRI sample, and fully eliminated when choice decomposition variables were added to simulated market-level sample models. Additionally, forecasting accuracy was much higher when using an aggregate NAcc activity classifier than using an aggregate vmPFC activity classifier, and this difference was particularly exacerbated when forecasting aggregate out-of-sample market level choices. In fact, despite attractiveness ratings playing a key role in explaining online dating choices at all levels of analysis, aggregate NAcc activity forecasts rivaled forecasting accuracy of aggregate attractiveness alone (33% accuracy for aggregate NAcc activity and 36% accuracy for aggregate attractiveness), but only when

neuroforecasting aggregate market-level choices. This illustrates the partial scaling value of aggregate NAcc activity, as an affective neural component, on forecasting aggregate out-of-sample choices (i.e., neuroforecasting). These results provide evidence for the argument that affective components of choice best scale to the aggregate, and in this context, self-reported ratings of attractiveness are in fact a highly effective behavioral indicator of the affective response to viewing online dating profiles.

One of the key arguments for the partial scaling account of NAcc activity scaling to the aggregate is that NAcc activity captures aspects of homogenous affective response to stimuli that prevail in markets. Researchers can subvert the natural variability of small samples and capture this homogeneity through observing NAcc activity and use these data to effectively forecast market outcomes. The forecasting results presented here provide support for this idea; forecasting accuracies for classifiers trained using fMRI sample aggregate NAcc activity were highest when forecasting market outcomes (32.5% accuracy), following by forecasting within fMRI sample outcomes (21.3% accuracy), and lowest when forecasting outcomes in the independent in-lab sample (17.6% accuracy). When neuroforecasting aggregate market choices, NAcc activity was highly useful, as per AIM and the partial scaling account of neuroforecasting, capturing the homogeneity in online dating choices observed in the large market sample, whereas when forecasting aggregate outcomes in the small in-lab sample (an independent behavioral sample), accuracies were quite poor as aggregate NAcc activity may not reflect the heterogeneity in small out of sample choice outcomes.

Predicting Individual Online Dating Outcomes. While NAcc activity at the individual level was most highly correlated with ratings of attractiveness, vmPFC activity was most highly correlated with perceptions of being liked back by the individual in the profile, an integrative

choice decomposition variable that takes into account a wide variety of choice related signals. Overall, the choice decomposition variables used in this study did an exceptional job of breaking down and predicting individual online dating choices. Although activity in the vmPFC was not independently predictive of individual-level binary online dating choices in regression models, vmPFC activity, but not NAcc activity, was consistently associated with increased likeback ratings, indicating the role of vmPFC activity in overall integrating measures of online dating decisions. This may indicate that developing isolated measures of integrative choice decomposition components is more challenging (at least in the context of online dating) than developing isolated measures of affective choice components (which attractiveness and personality do quite effectively in the context of online dating). That said, results indicated that activity in the NAcc and vmPFC did in fact significantly contribute to prediction of individual-level choice over and above the choice decomposition variables within-sample. This finding, in combination with the result that adding vmPFC activity alone produced the greatest increase in individual choice prediction accuracy over and above classifiers with choice decomposition variables, suggests that vmPFC activity indeed is useful for understanding individual choices in the context of online dating.

Finally, observing the relationship between the likeback variable and vmPFC activity can help us understand the relationship between the role of integrative components in this study. Interestingly, vmPFC activity was robustly associated with individual likeback ratings regardless of the inclusion or exclusion of choice decomposition or factorial variables, but when looking at the relationship between these two variables at the aggregate level, the association persists within sample but not when using market likeback rates. That is, we observe the association between integrative components vmPFC activity and likeback at the individual level and within sample,

but not at the aggregate market level, which is further evidence that vmPFC activity is most useful for ether individual level prediction or within sample forecasting, but not neuroforecasting per se (in this context).

Behavioral Variables as Proxies for Neural Processes. Given the cost and labor associated with collecting neuroimaging data, a key consideration when attempting to forecast is whether neural data is worth collecting in a given context. Several pieces of evidence in the present study suggest that if behavioral variables are adequately prespecified to map to components in the AIM framework, highly accurate out-of-sample market forecasts can be achieved without the use of neural data. Supplementarily, it may be cost effective to use neuroimaging to confirm, via correlation and/ or association, the type of information that behavioral variables are collecting in a given set of contexts, based on pre-specified hypotheses. Marketers can then proceed to use these variables, along with the tenets of AIM, for prediction and forecasting, rather than needing to collect neural data in each context and/ or needing neural data to produce the highest accuracy forecasts. This was the case with the attractiveness variable in the present study – attractiveness served as an accurate proxy of affective neural activity in the NAcc, and could be used to effectively forecast aggregate choices. That said, other prior studies have shown that vmPFC activity can be more effective at neuroforecasting aggregate outcomes in some contexts (Falk et al., 2016), and further research is needed to elucidate the contexts and outcome types that may rely more heavily on the contribution of the value integration component of the AIM framework to prediction and forecasting.

In the context of online dating, we observed that although several choice decomposition variables, which served as proxies for affective and value integrative components of the AIM framework, were valuable in understanding and predicting individual choices, the primary

affective component of choice, attractiveness, was essential to understanding and forecasting market outcomes. By deconstructing the choice process and using the AIM framework as a foundation for our theorizing, we were able to pre-specify that attractiveness would be a key element to forecasting aggregate market choices. This account is consistent with a partial scaling account of aggregate forecasting, as only some, but not all components of individual choice (namely, the affective components of attractiveness and personality) improved aggregate forecasting accuracies, while others did not. With this knowledge, marketers may in fact choose to train classifiers and make forecasts using only aggregation of variables that represent affective processes when attempting to forecast aggregate market choices, as (at least in the present context) these components alone produced better forecasting accuracy than models including all choice decomposition variables combined. Without evidence from the neuroforecasting literature, the AIM framework as a foundation, and support for a partial scaling account of forecasting aggregate choices across a number of contexts, such a recommendation or course of action would be unlikely, as it would be typical to include all variables used to understand choices in forecasting models.

Conclusion

The findings of the present study provide initial support for the AIM framework as a foundation for understanding the applications of neuroforecasting. First, we were able to neuroforecast aggregate online dating choices using activity from the NAcc, providing evidence in a novel context that while both affective and value integration components of the decision-making process can be powerful tools for understanding and predicting individual choice, affective components seem to translate through most effectively when attempting to understand or forecast aggregate outcomes (in particular, at the market level). Second, we provide support

for the idea that, in certain contexts, if choice decomposition variables can be effectively mapped to the components of the AIM framework (namely, choice decomposition variables that represent affective and value integration phases of AIM), behavioral data can produce excellent predictions of individual choice and forecasts of aggregate choice. With that said, an important implication of this research is that marketing researchers and practitioners alike who do not have access to neuroscientific tools or have limited budgeting constraints can still take advantage of findings from consumer neuroscience.

REFERENCES

Abraham, A., Pedregosa, F., Eickenberg, M., Gervais, P., Mueller, A., Kossaifi, J., Gramfort, A., Thirion, B., & Varoquaux, G. (2014). Machine learning for neuroimaging with scikit-learn. *Frontiers in Neuroinformatics*, *8*(FEB), 14.

Andy's Brain Book 1.0 documentation - SPM Tutorial #9: ROI Analysis. (2020). Retrieved August 9, 2021, from https://andysbrainbook.readthedocs.io/en/latest/SPM/SPM_Short_Course/SPM_09_ROIAnalysis.html

Bechara, A., Damasio, H., Damasio, A. R., & Lee, G. P. (1999). Different contributions of the human amygdala and ventromedial prefrontal cortex to decision-making. *Journal of Neuroscience*, *19*(13), 5473–5481.

Bechara, A., Tranel, D., Damasio, H., & Damasio, A. R. (1996). Failure to respond autonomically to anticipated future outcomes following damage to prefrontal cortex. *Cerebral Cortex*, *6*(2), 215–225.

Behzadi, Y., Restom, K., Liau, J., & Liu, T. T. (2007). A component based noise correction method (CompCor) for BOLD and perfusion based fMRI. *NeuroImage*, *37*(1), 90–101.

Bernheim, B. D. (2009). The psychology and neurobiology of judgment and decision making: What's in it for economists? In *Neuroeconomics* (pp. 113–125). Elsevier Inc.

Berns, G. S., & Moore, S. E. (2012). A neural predictor of cultural popularity. *Journal of Consumer Psychology*, *22*(1), 154–160.

Yale BioImage Suite MNI<->TAL. (2020). Retrieved July 1, 2021, from https://bioimagesuiteweb.github.io/webapp/mni2tal.html

Brett, M., Anton, J.-L., Valabregue, R., & Poline, J.-B. (n.d.). Presented at the 8th International Conferance on Functional Mapping of the Human Brain. In *Japan. Available on CD-ROM in NeuroImage* (Vol. 16). Retrieved April 19, 2021, from http://www.mrc-cbu.cam.ac.uk/Imaging/marsbar.html

Büchel, C., & Dolan, R. J. (2000). Classical fear conditioning in functional neuroimaging. In *Current Opinion in Neurobiology* (Vol. 10, Issue 2, pp. 219–223). Current Biology Ltd.

Carnevale, A., Cheah, B., & Hanson, A. (2015). *The economic value of college majors*. https://repository.library.georgetown.edu/handle/10822/1050288

Chandler, J. (2018). Likeableness and meaningfulness ratings of 555 (+487) person-descriptive words. *Journal of Research in Personality*, *72*, 50–57.

Cox, R. W. (1996). AFNI: Software for analysis and visualization of functional magnetic resonance neuroimages. *Computers and Biomedical Research*, *29*(3), 162–173.

Esteban, O., Birman, D., Schaer, M., Koyejo, O. O., Poldrack, R. A., & Gorgolewski, K. J. (2017). MRIQC: Advancing the automatic prediction of image quality in MRI from unseen sites. *PLOS ONE*, *12*(9), e0184661.

Esteban, O., Markiewicz, C. J., Goncalves, M., DuPre, E., Kent, J. D., Salo, T., Ciric, R., Pinsard, B., Blair, R. W., Poldrack, R. A., & Gorgolewski, K. J. (2020). *fMRIPrep: a robust preprocessing pipeline for functional MRI*.

Falk, E. B., Berkman, E. T., & Lieberman, M. D. (2012). From Neural Responses to Population Behavior: Neural Focus Group Predicts Population-Level Media Effects. *Psychological Science*, *23*(5), 439-445.

Falk, E. B., O'Donnell, M. B., Tompson, S., Gonzalez, R., Dal Cin, S., Strecher, V., Cummings, K. M., & An, L. (2016). Functional brain imaging predicts public health campaign success. *Social Cognitive and Affective Neuroscience*, *11*(2), 204–214.

Fama, E. F. (1970). Efficient Capital Markets: A Review of Theory and Empirical Work. *The Journal of Finance*, *25*(2), 383.

Fisman, R., Iyengar, S. S., Kamenica, E., & Simonson, I. (2008). Racial Preferences in Dating. *The Review of Economic Studies*, *75*(1), 117–132.

Fonov, V., Evans, A., McKinstry, R., Almli, C., & Collins, D. (2009). Unbiased nonlinear average age-appropriate brain templates from birth to adulthood. *NeuroImage*, *47*, S102.

Genevsky, A., & Knutson, B. (2015). Neural affective mechanisms predict market-level microlending. *Psychological Science*. *26*(9), 1411-1422.

Genevsky, A., Yoon, C., & Knutson, B. (2017). When Brain Beats Behavior: Neuroforecasting Crowdfunding Outcomes. *Journal of Neuroscience*, *37*(36), 8625–8634.

Gorgolewski, K. J., Auer, T., Calhoun, V. D., Craddock, R. C., Das, S., Duff, E. P., Flandin, G., Ghosh, S. S., Glatard, T., Halchenko, Y. O., Handwerker, D. A., Hanke, M., Keator, D., Li, X., Michael, Z., Maumet, C., Nichols, B. N., Nichols, T. E., Pellman, J., … Poldrack, R. A.

(2016). The brain imaging data structure, a format for organizing and describing outputs of neuroimaging experiments. *Scientific Data*, *3*(1), 1–9.

Gorgolewski, K., Burns, C. D., Madison, C., Clark, D., Halchenko, Y. O., Waskom, M. L., & Ghosh, S. S. (2011). Nipype: A Flexible, Lightweight and Extensible Neuroimaging Data Processing Framework in Python. *Frontiers in Neuroinformatics*, *5*, 13.

Greve, D. N., & Fischl, B. (2009). Accurate and robust brain image alignment using boundary-based registration. *NeuroImage*, *48*(1), 63–72.

Highest Paying Occupations : Occupational Outlook Handbook: : U.S. Bureau of Labor Statistics. (2020). Retrieved April 19, 2021, from https://www.bls.gov/ooh/highest-paying.htm

Jenkinson, M., Bannister, P., Brady, M., & Smith, S. (2002). Improved Optimization for the Robust and Accurate Linear Registration and Motion Correction of Brain Images. *NeuroImage*, *17*(2), 825–841.

Jenkinson, M., Beckmann, C. F., Behrens, T. E. J., Woolrich, M. W., & Smith, S. M. (2012). FSL. *NeuroImage*, *62*(2), 782–790.

Knutson, B., Adams, C. M., Fong, G. W., & Hommer, D. (2001). Anticipation of increasing monetary reward selectively recruits nucleus accumbens. *The Journal of Neuroscience : The Official Journal of the Society for Neuroscience*, *21*(16).

Knutson, B., & Genevsky, A. (2018). Neuroforecasting Aggregate Choice. *Current Directions in Psychological Science*. *27*(2), 110-115.

Knutson, B., Rick, S., Wimmer, G. E., Prelec, D., & Loewenstein, G. (2007). Neural Predictors of Purchases. *Neuron*, *53*(1), 147–156.

Koenigs, M., & Tranel, D. (2008). Prefrontal cortex damage abolishes brand-cued changes in cola preference. *Social Cognitive and Affective Neuroscience*, *3*(1), 1-6.

Kuhn, M. (2008). Building predictive models in R using the caret package. *Journal of Statistical Software*, *28*(5), 1–26.

Kühn, S., Strelow, E., & Gallinat, J. (2016). Multiple "buy buttons" in the brain: Forecasting chocolate sales at point-of-sale based on functional brain activation using fMRI. *NeuroImage*, *136*, 122–128.

Kuhnen, C. M., & Knutson, B. (2005). The neural basis of financial risk taking. *Neuron*, *47*(5), 763–770.

Levy, D. J., & Glimcher, P. W. (2012). The root of all value: a neural common currency for choice. *Current Opinion in Neurobiology*, *22*(6), 1027–1038.

Ma, D. S., Correll, J., & Wittenbrink, B. (2015). The Chicago face database: A free stimulus set of faces and norming data. *Behavior Research Methods*, *47*(4), 1122–1135.

MATLAB - MathWorks - MATLAB & Simulink. (n.d.). Retrieved April 19, 2021, from https://www.mathworks.com/products/matlab.html

McClintock, E. A. (2010). When Does Race Matter? Race, Sex, and Dating at an Elite University. *Journal of Marriage and Family*, *72*(1), 45–72.

NITRC: REX: Tool/Resource Info. (n.d.). Retrieved April 19, 2021, from https://www.nitrc.org/projects/rex/

Ogawa, S., Lee, T. -M, Nayak, A. S., & Glynn, P. (1990). Oxygenation-sensitive contrast in magnetic resonance image of rodent brain at high magnetic fields. *Magnetic Resonance in Medicine*, *14*(1), 68–78.

Paulus, M. P., Rogalsky, C., Simmons, A., Feinstein, J. S., & Stein, M. B. (2003). Increased activation in the right insula during risk-taking decision making is related to harm avoidance and neuroticism. *NeuroImage*, *19*(4), 1439–1448.

Paulus, M. P., & Stein, M. B. (2006). An Insular View of Anxiety. In *Biological Psychiatry* (Vol. 60, Issue 4, pp. 383–387). Biol Psychiatry.

Plassmann, H., Ambler, T., & Braeutigam, S. (2007). What can advertisers learn from neuroscience? *International Journal of Advertising, 26*(2), 151–175.

Plassmann, H., O'Doherty, J., Shiv, B., & Rangel, A. (2008). Marketing actions can modulate neural representations of experienced pleasantness. *Proceedings of the National Academy of Sciences*, *105*(3), 1050–1054.

polr function - RDocumentation. (n.d.). Retrieved April 19, 2021, from https://www.rdocumentation.org/packages/MASS/versions/7.3-53.1/topics/polr

Popular Baby Names. (2020). Retrieved April 19, 2021, from https://www.ssa.gov/OACT/babynames/index.html

Power, J. D., Mitra, A., Laumann, T. O., Snyder, A. Z., Schlaggar, B. L., & Petersen, S. E. (2014). Methods to detect, characterize, and remove motion artifact in resting state fMRI. *NeuroImage*, *84*, 320–341.

Psychology Software Tools, Inc. [E-Prime 3.0]. (2020). Retrieved from https://support.pstnet.com/

Samanez-Larkin, G. R., & Knutson, B. (2014). Reward processing and risky decision making in the aging brain. In *The neuroscience of risky decision making.* (pp. 123–142). American Psychological Association.

SPM - Statistical Parametric Mapping. (n.d.). Retrieved April 19, 2021, from https://www.fil.ion.ucl.ac.uk/spm/

Tong, L. C., Yavuz Acikalin, M., Genevsky, A., Shiv, B., & Knutson, B. (2020). Brain activity forecasts video engagement in an internet attention market. *Proceedings of the National Academy of Sciences of the United States of America*, *117*(12), 6936–6941.

Tusche, A., Bode, S., & Haynes, J.-D. (2010). Neural Responses to Unattended Products Predict Later Consumer Choices. *Journal of Neuroscience*, *30*(23), 8024–8031.

Tustison, N. J., Avants, B. B., Cook, P. A., Zheng, Y., Egan, A., Yushkevich, P. A., & Gee, J. C. (2010). N4ITK: Improved N3 bias correction. *IEEE Transactions on Medical Imaging*, *29*(6), 1310–1320.

Venkatraman, V., Dimoka, A., Pavlou, P. A., Vo, K., Hampton, W., Bollinger, B., Hershfield, H. E., Ishihara, M., & Winer, R. S. (2015). Predicting Advertising Success Beyond Traditional Measures: New Insights from Neurophysiological Methods and Market Response Modeling. *Journal of Marketing Research*, *52*(4), 436–452.

Von Neumann, J., & Morgenstern, O. (1944). Theory of games and economic behavior. Princeton University Press.

Yoon, C., Gutchess, A. H., Feinberg, F., & Polk, T. A. (2006). A Functional Magnetic Resonance Imaging Study of Neural Dissociations between Brand and Person Judgments. *Journal of Consumer Research*, *33*(1), 31–40.

Zhang, Y., Brady, M., & Smith, S. (2001). Segmentation of brain MR images through a hidden Markov random field model and the expectation-maximization algorithm. *IEEE Transactions on Medical Imaging*, *20*(1), 45–57.

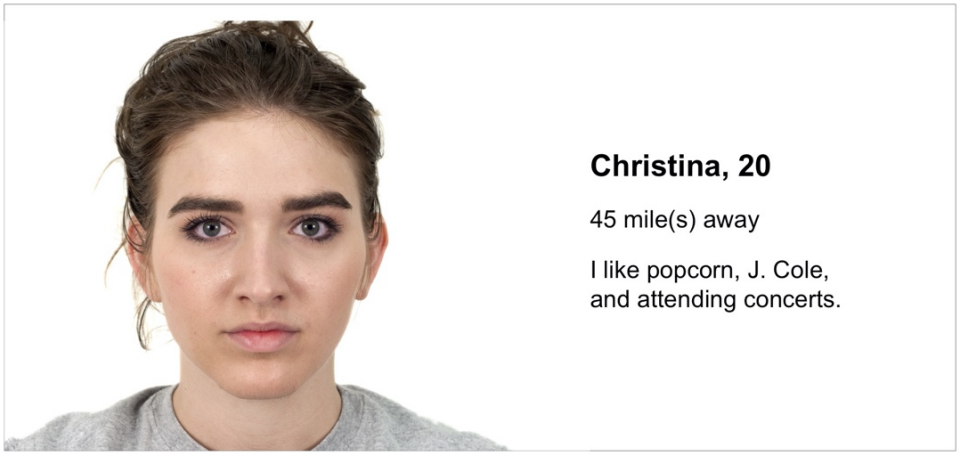

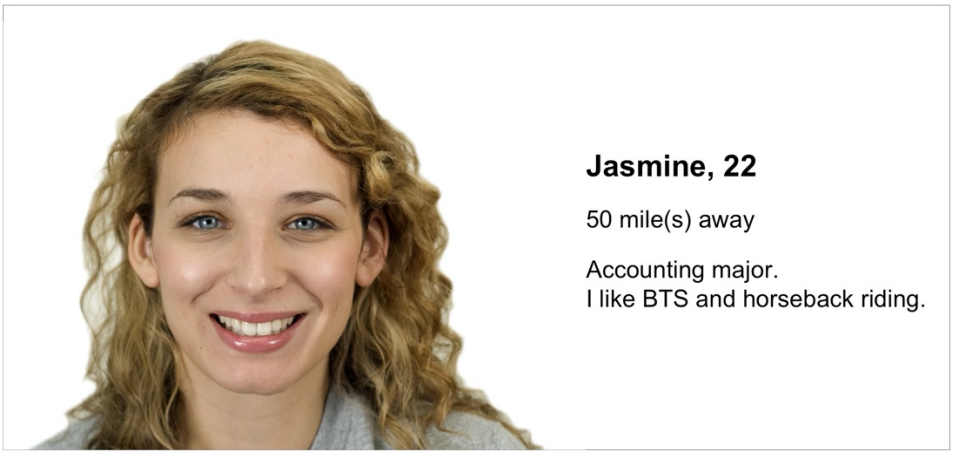

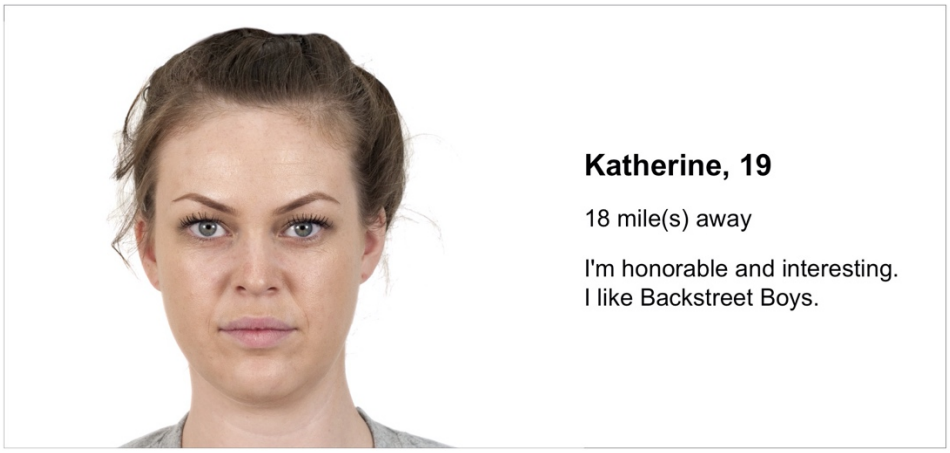

Figure 2.1. Three example online dating profile stimuli. Top profile characteristics: high attractiveness, 18-23 age bin, neutral facial expression, and hobbies/interests profile description. Middle profile characteristics: medium attractiveness, 18-23 age bin, smiling facial expression, and SES/ career indicator profile description. Bottom profile characteristics: low attractiveness, 18-23 age bin, neutral facial expression, and personality traits profile description.

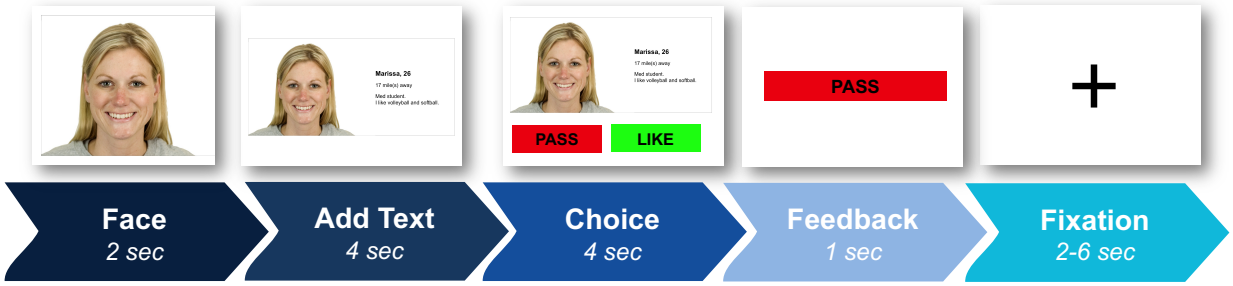

Figure 2.2. Task design and timing of stimuli presentation inside of the fMRI scanner. Profiles were presented in random order and like and pass button locations were switched randomly between trials. Feedback was given immediately upon button press during the choice phase, and any remaining time in the choice phase was added to the fixation stage.

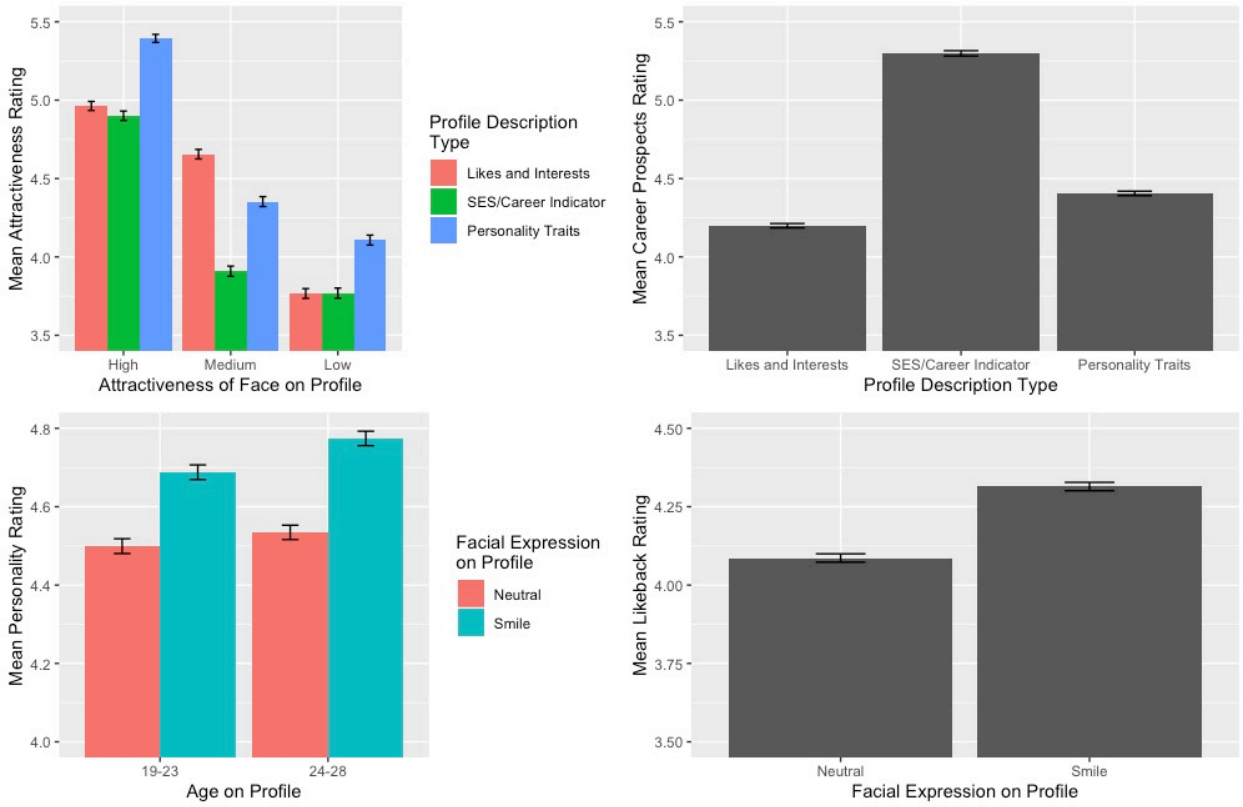

Figure 2.3. Bar graphs illustrating descriptive statistics of interest for each dependent variable in the simulated market sample. Top left panel: participants' attractiveness ratings are mainly determined by attractiveness of the facial image on each profile, however, profile description clearly influences attractiveness ratings within each level of profile facial attractiveness. Top right panel: the SES/career indicator in a profile description clearly increases participant's perceptions of the career prospects of the individual in a profile. Bottom left panel: age on the profile does not influence participant's ratings of personality for profiles, but if the individual in the profile is smiling, participant's rate that individual as having a more likeable personality. Bottom right panel: if the individual in a profile is smiling, participants are more likely to believe that the individual in the profile would 'like' them back.

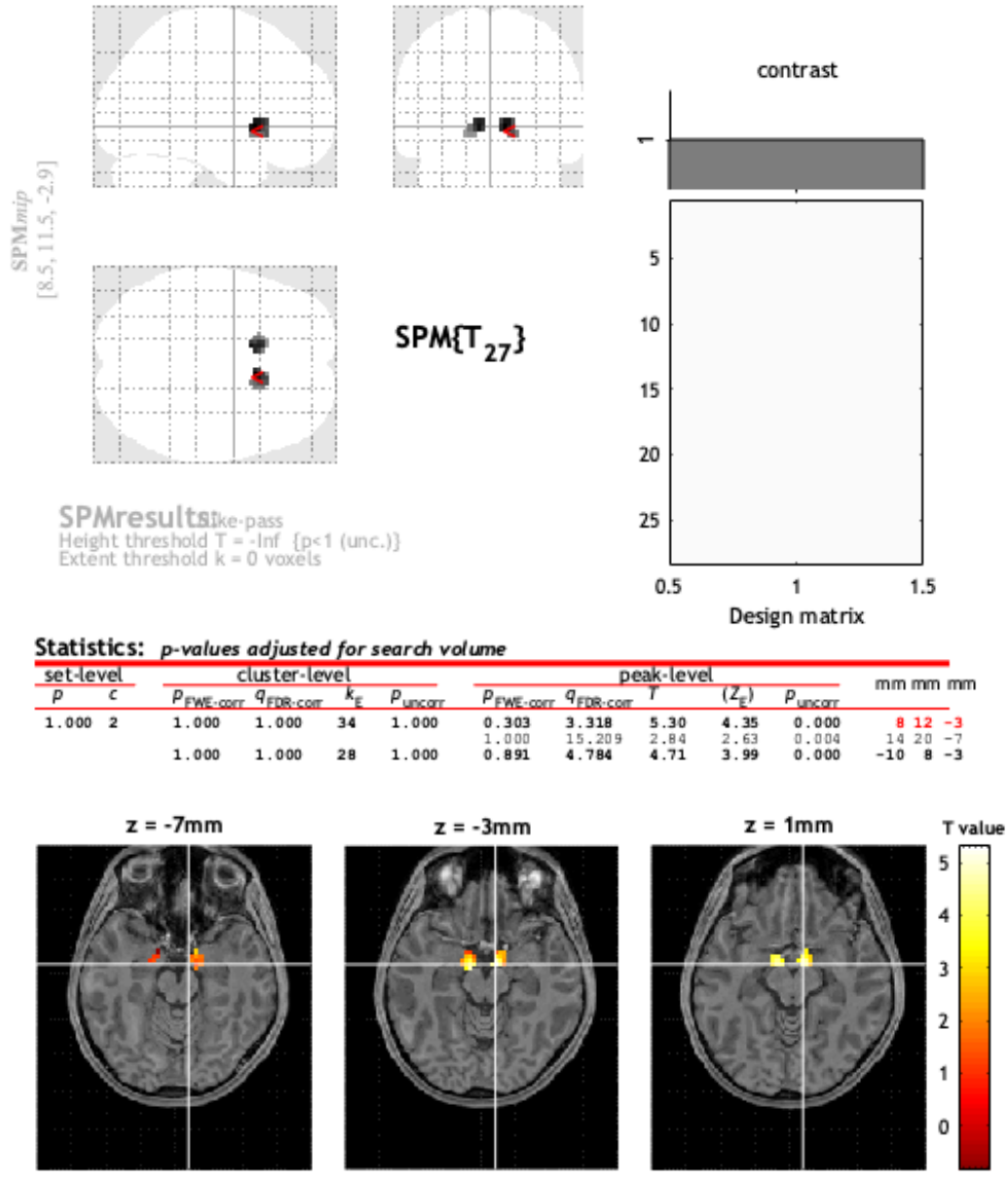

Figure 2.4. Brain activity in the NAcc when contrasting liked minus passed dating profiles.

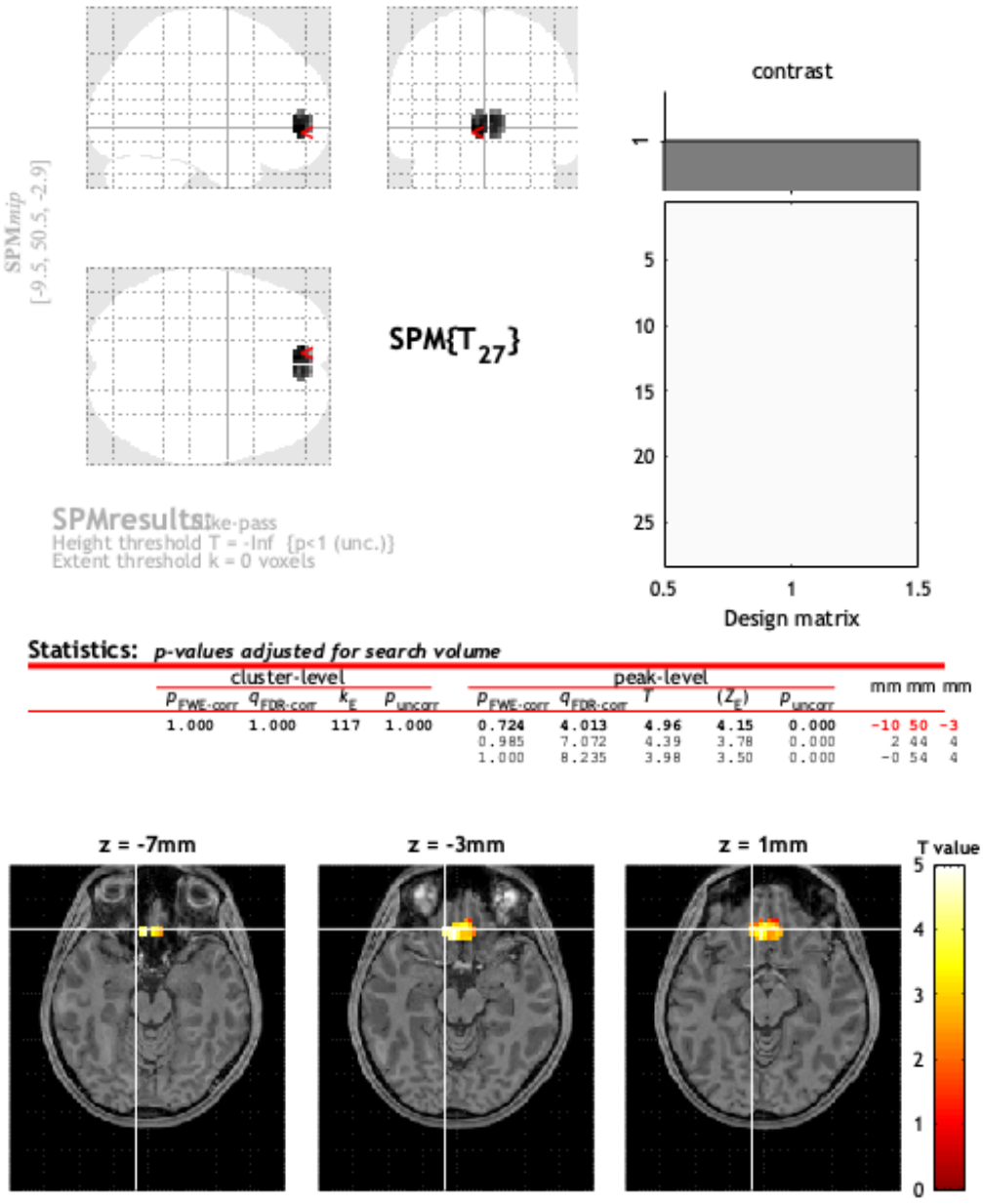

Figure 2.5. Brain activity in the vmPFC when contrasting liked minus passed dating profiles.

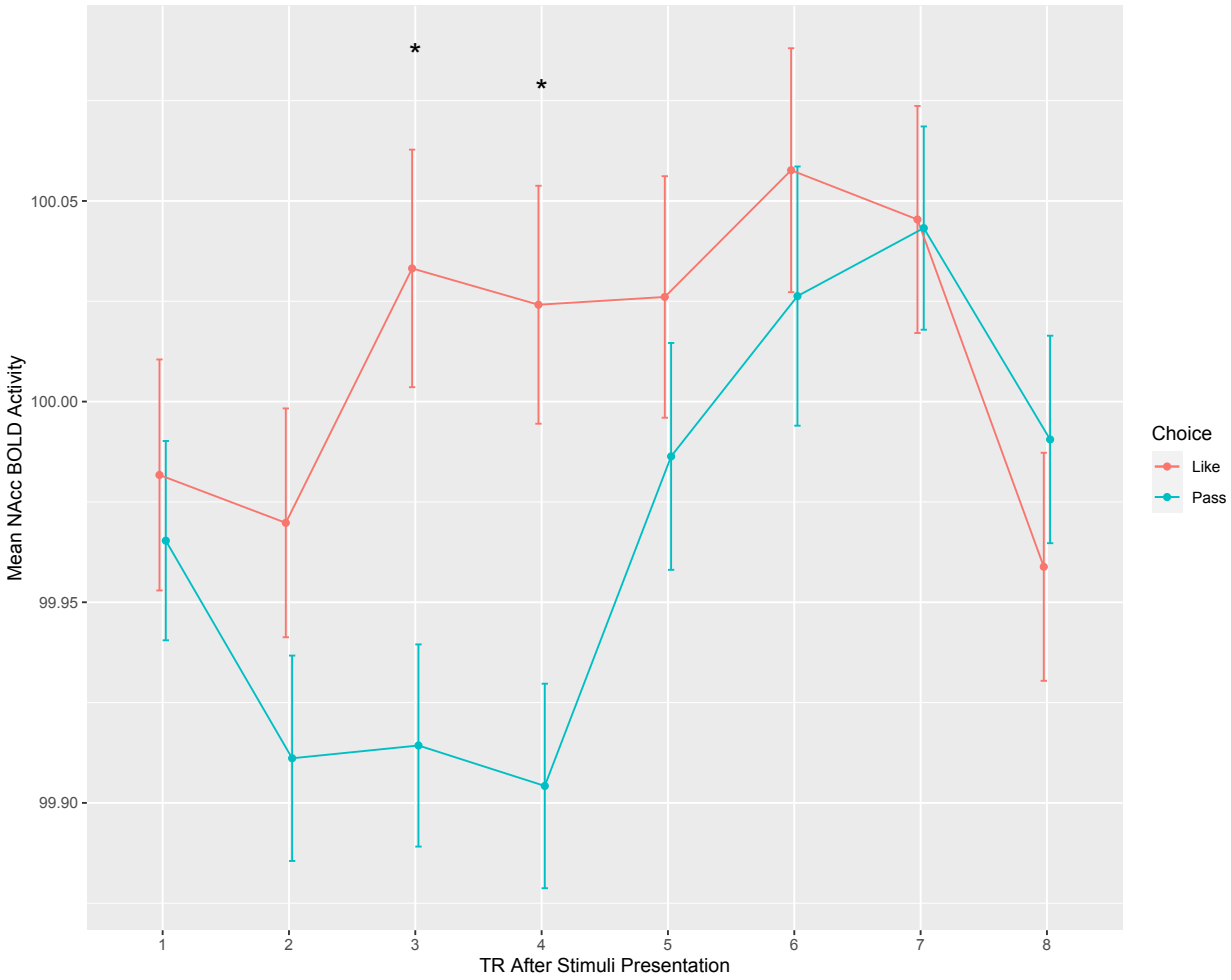

Figure 2.6. Mean NAcc BOLD brain activity time course following stimuli presentation onset for online dating profiles that were liked versus those that were passed. Activity in the NAcc was significantly higher for liked profiles at TR 3 and 4 (* indicated significance at a threshold of $p < 0.05$).

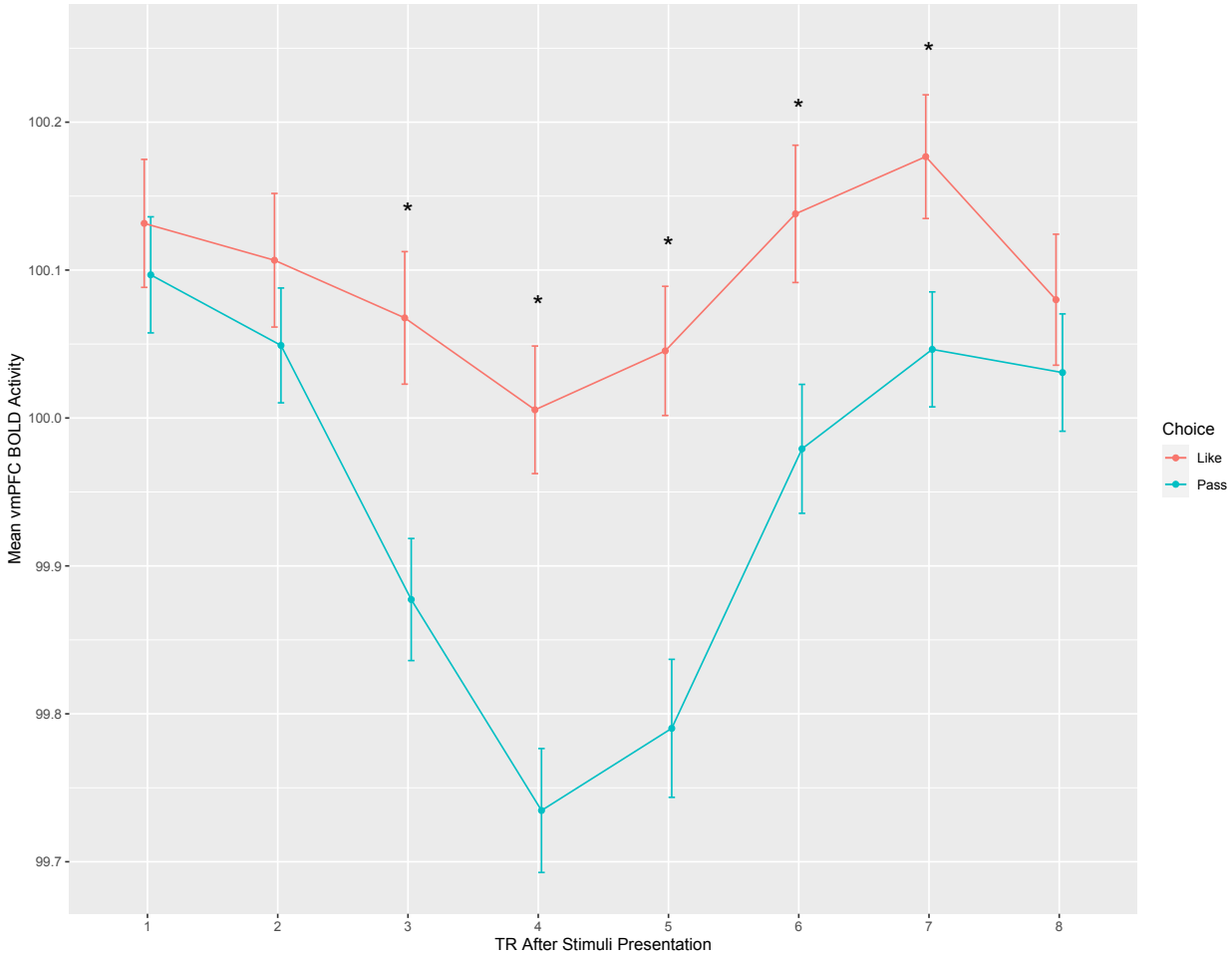

Figure 2.7. Mean vmPFC BOLD brain activity time course following stimuli presentation onset for online dating profiles that were liked versus those that were passed. Activity in the NAcc was significantly higher for liked profiles at TR 3 through 7 (* indicated significance at a threshold of $p < 0.05$).

	Dependent variable:				
	Choice	Attractive	Career	Personality	Likeback
	logistic	*OLS*	*OLS*	*OLS*	*OLS*
	(1)	(2)	(3)	(4)	(5)
Attractiveness_bin (Medium)	−0.841***	−0.593***	−0.232***	−0.140***	−0.021
	(0.033)	(0.014)	(0.014)	(0.015)	(0.015)
Attractiveness_bin (Low)	−1.417***	−0.922***	−0.301***	−0.458***	−0.208***
	(0.034)	(0.014)	(0.014)	(0.015)	(0.015)
Facial Expression (Smiling)	−0.210***	−0.196***	0.042***	0.195***	0.210***
	(0.027)	(0.012)	(0.012)	(0.013)	(0.012)
Age (24-28)	0.078***	0.004	−0.006	0.061***	0.057***
	(0.027)	(0.012)	(0.012)	(0.013)	(0.012)
Profile Description (SES/Career)	−0.239***	−0.209***	0.981***	−0.106***	−0.078***
	(0.033)	(0.014)	(0.014)	(0.015)	(0.015)
Profile Description (Personality)	0.285***	0.124***	0.171***	0.111***	0.080***
	(0.033)	(0.014)	(0.014)	(0.015)	(0.015)
Constant	0.744***	0.629***	−0.224***	0.070***	−0.058***
	(0.036)	(0.016)	(0.015)	(0.017)	(0.016)
Observations	23,544	23,544	23,544	23,544	23,544
R^2		0.176	0.202	0.056	0.026
Adjusted R^2		0.175	0.202	0.056	0.026
Log Likelihood	−15,239.020				
Akaike Inf. Crit.	30,492.030				
Residual Std. Error (df = 23537)		0.904	0.889	0.961	0.955
F Statistic (df = 6; 23537)		835.692***	993.172***	233.654***	106.392***

Note: n = 654, 36 profiles per participant *p<0.1; **p<0.05; ***p<0.01

Table 2.1. Logistic and OLS regression results showing the effect of profile design factorial elements on overall choice and choice decomposition variables in the simulated market data. Individual-level simulated market data.

	Dependent variable:					
	Binary Choice ('Like' vs. 'Pass')					
	(1)	(2)	(3)	(4)	(5)	(6)
Attractiveness Ratings	1.867***	1.865***	1.704***	1.702***	1.658***	1.655***
	(0.030)	(0.030)	(0.031)	(0.031)	(0.032)	(0.032)
Career Prospect Ratings	0.195***	0.195***	0.284***	0.284***	0.275***	0.276***
	(0.023)	(0.023)	(0.028)	(0.028)	(0.028)	(0.029)
Personality Ratings	0.730***	0.729***	0.740***	0.740***	0.725***	0.725***
	(0.027)	(0.027)	(0.028)	(0.028)	(0.028)	(0.028)
Likeback Ratings	0.491***	0.490***	0.527***	0.527***	0.528***	0.528***
	(0.026)	(0.026)	(0.027)	(0.027)	(0.027)	(0.027)
Self-rated Attractiveness		0.058		0.061		0.060
		(0.098)		(0.101)		(0.102)
Participant Age		0.042**		0.043**		0.043**
		(0.019)		(0.019)		(0.019)
Attractiveness_bin (Medium)			−0.576***	−0.579***	−0.653***	−0.655***
			(0.054)	(0.054)	(0.151)	(0.152)
Attractiveness_bin (Low)			−0.887***	−0.886***	−1.005***	−1.003***
			(0.057)	(0.057)	(0.152)	(0.153)
Facial Expression (Smiling)			−0.385***	−0.386***	−0.389***	−0.390***
			(0.045)	(0.045)	(0.124)	(0.124)
Age (24-28)			0.162***	0.160***	0.178	0.177
			(0.043)	(0.043)	(0.123)	(0.123)
Profile Description (SES/Career)			−0.293***	−0.295***	−0.324**	−0.325**
			(0.061)	(0.061)	(0.154)	(0.154)
Profile Description (Personality)			0.250***	0.248***	0.279*	0.276*
			(0.053)	(0.053)	(0.151)	(0.151)
Constant	−0.183*	−1.287**	0.425***	−0.703	0.484**	−0.661
	(0.098)	(0.505)	(0.114)	(0.519)	(0.191)	(0.548)
Observations	23,544	23,508	23,544	23,508	23,544	23,508
Log Likelihood	−8,147.459	−8,133.167	−7,950.208	−7,936.311	−7,876.417	−7,862.408
Akaike Inf. Crit.	16,306.920	16,282.330	15,924.420	15,900.620	15,778.830	15,754.820
Bayesian Inf. Crit.	16,355.320	16,346.860	16,021.220	16,013.530	15,883.700	15,875.790
Note: n = 654	Random effects, m1-m4 ResponseId; m5/m6 RId + stim; *p<0.1; **p<0.05; ***p<0.01					

Table 2.2. Logistic regression results with robustness checks, showing the effect of choice decomposition variables on choice in the simulated market data. Model 6 is the full model, including all control variables and random effects. Individual-level simulated market data.

	Attractiveness	Career Prospects	Personality	Likeback	Attractiveness bin	Facial Expression	Age bin
Attractiveness							
Career Prospects	0.212****						
Personality	0.398****	0.268****					
Likeback	0.165****	0.129****	0.394****				
Attractiveness bin	-0.468****	-0.138****	-0.231****	-0.060*			
Facial Expression	-0.124****	0.042	0.131****	0.123****	0		
Age bin	0.035	-0.037	0.020	-0.042	0	0	
Profile Description	0.043	0.084***	0.053*	0.062*	0	0	0
Note: n = 45						*p<0.05; **p<0.01; ***p<0.001; ****p<0.0001	

Table 2.3. Individual-level correlations between choice decomposition variables and factorial design elements in the in-lab sample.

	Attractiveness	Career Prospects	Personality	Likeback	Attractiveness bin	Facial Expression	Age bin	Profile Description	NAcc
Attractiveness									
Career Prospects	0.067*								
Personality	0.355****	0.109***							
Likeback	0.113***	0.052	0.319****						
Attractiveness bin	-0.498****	-0.139****	-0.197****	-0.023					
Facial Expression	-0.141****	0.054	0.124****	0.102***	0				
Age bin	-0.034	-0.018	0.093**	-0.036	0	0			
Profile Description	0.051	0.085**	-0.018	0.012	0	0	0		
NAcc	0.151****	-0.020	0.088**	0.101**	-0.073*	-0.027	-0.024	-0.003	
vmPFC	0.037	0.016	0.056	0.106***	-0.022	0.025	0.007	-0.042	0.420****

Note: n = 29 *p<0.05; **p<0.01; ***p<0.001; ****p<0.0001

Table 2.4. Individual-level correlations between choice decomposition variables and factorial design elements in the fMRI sample.

	Attractiveness	Career Prospects	Personality	Likeback	Attractiveness bin	Facial Expression	Age bin
Attractiveness							
Career Prospects	0.228****						
Personality	0.432****	0.285****					
Likeback	0.283****	0.212****	0.443****				
Attractiveness bin	-0.378****	-0.123****	-0.189****	-0.088****			
Facial Expression	-0.099****	0.021**	0.098****	0.108****	0		
Age bin	0.002	-0.003	0.031****	0.030****	0	0	
Profile Description	0.051****	0.070****	0.046****	0.034****	0	0	0
Note: n = 654							*p<0.05; **p<0.01; ***p<0.001; ****p<0.0001

Table 2.5. Individual-level correlations between choice decomposition variables and factorial design elements in the simulated market sample.

	Dependent variable:		
	Binary Choice ('Like' vs. 'Pass')		
	(1)	(2)	(3)
Attractiveness Ratings	2.845**		2.696**
	(0.171)		(0.174)
Career Prospects Ratings	0.196		0.152
	(0.102)		(0.122)
Personality Ratings	0.691**		0.705**
	(0.120)		(0.125)
Likeback Ratings	0.918**		0.923**
	(0.121)		(0.123)
Attractiveness_bin (Medium)		−1.698**	−0.723**
		(0.153)	(0.244)
Attractiveness_bin (Low)		−2.322**	−0.979**
		(0.167)	(0.260)
Facial Expression (Smiling)		−0.254*	−0.245
		(0.126)	(0.204)
Age (24-28)		−0.159	−0.426*
		(0.126)	(0.199)
Profile Description (SES/Career)		−0.086	0.097
		(0.156)	(0.277)
Profile Description (Personality)		0.420**	0.200
		(0.153)	(0.239)
Self-rated Attractiveness	−0.957*	−0.423*	−0.970*
	(0.411)	(0.187)	(0.408)
Participant Age	0.329	0.131	0.333**
	(0.168)	(0.077)	(0.008)
Constant	−8.821*	−2.145	−8.140**
	(3.496)	(1.594)	(0.505)
Log Likelihood	−424.309	−816.293	−413.147
Akaike Inf. Crit.	864.618	1,652.587	854.294
Bayesian Inf. Crit.	907.740	1,706.489	929.757
Note: n = 45, observations = 1,620			*p<0.05; **p<0.01

Table 2.6. In-lab sample individual level logistic regression results for binary choice regressed on choice decomposition variables (1) and profile factorial elements (2), as separately and combined (3). All models contain participant ID random effects.

	Dependent variable:					
	Binary Choice ('Like' vs. 'Pass')					
	(1)	(2)	(3)	(4)	(5)	(6)
Attractiveness Ratings	1.217**			1.196**		1.015**
	(0.100)			(0.100)		(0.112)
Career Prospects Ratings	−0.129			−0.129		0.030
	(0.088)			(0.088)		(0.123)
Personality Ratings	0.678**			0.683**		0.698**
	(0.094)			(0.095)		(0.102)
Likeback Ratings	0.168			0.138		0.156
	(0.091)			(0.092)		(0.094)
Attractiveness_bin (Medium)		−1.066**			−1.064**	−0.403
		(0.171)			(0.174)	(0.208)
Attractiveness_bin (Low)		−1.795**			−1.782**	−0.578*
		(0.184)			(0.186)	(0.229)
Facial Expression (Smiling)		−0.472**			−0.474**	−0.531**
		(0.143)			(0.145)	(0.172)
Age (24-28)		−0.133			−0.125	−0.229
		(0.142)			(0.144)	(0.168)
Profile Description (SES/Career)		−0.969**			−0.968**	−0.692*
		(0.179)			(0.181)	(0.275)
Profile Description (Personality)		−0.163			−0.149	−0.312
		(0.170)			(0.172)	(0.200)
NAcc			0.404**	0.212	0.343**	0.208
			(0.102)	(0.126)	(0.111)	(0.129)
vmPFC			0.052	0.061	0.072	0.065
			(0.034)	(0.041)	(0.037)	(0.043)
Log Likelihood	−494.36	−605.60	−666.68	−490.22	−594.46	−478.25
Akaike Inf. Crit.	1,004.71	1,231.21	1,345.36	1,000.44	1,212.92	988.50
Bayesian Inf. Crit.	1,044.30	1,280.69	1,375.05	1,049.92	1,272.30	1,067.67
Note: n = 29, observations = 1,042						*p<0.05; **p<0.01

Table 2.7. Individual-level logistic regression results showing the effect of vmPFC and NAcc on binary choice in the fMRI sample. All models include participant age and self-rated attractiveness control variables and participant ID random effects.

	Dependent variable:					
	Likeback (7-point Likert)					
	(1)	(2)	(3)	(4)	(5)	(6)
Attractiveness Ratings	−0.001			−0.008		0.024
	(0.030)			(0.030)		(0.035)
Career Prospects Ratings	0.017			0.018		0.037
	(0.029)			(0.028)		(0.038)
Personality Ratings	0.300**			0.295**		0.286**
	(0.030)			(0.030)		(0.031)
Attractiveness_bin (Medium)		−0.014			−0.006	0.091
		(0.071)			(0.071)	(0.073)
Attractiveness_bin (Low)		−0.054			−0.039	0.138
		(0.072)			(0.071)	(0.079)
Facial Expression (Smiling)		0.193**			0.193**	0.125*
		(0.058)			(0.058)	(0.057)
Age (24-28)		−0.069			−0.067	−0.117*
		(0.058)			(0.058)	(0.056)
Profile Description (SES/Career)		−0.104			−0.100	−0.041
		(0.071)			(0.071)	(0.089)
Profile Description (Personality)		0.028			0.036	0.036
		(0.071)			(0.071)	(0.068)
NAcc			0.084*	0.057	0.080	0.055
			(0.041)	(0.040)	(0.041)	(0.040)
vmPFC			0.032*	0.028*	0.032*	0.029*
			(0.014)	(0.013)	(0.014)	(0.013)
Log Likelihood	−1,379.245	−1,429.840	−1,424.936	−1,379.511	−1,427.685	−1,383.616
Akaike Inf. Crit.	2,774.490	2,881.680	2,863.871	2,779.023	2,881.369	2,799.232
Bayesian Inf. Crit.	2,814.073	2,936.107	2,898.507	2,828.502	2,945.692	2,878.399

Note: n = 29, observations = 1,041 *p<0.05; **p<0.01

Table 2.8. Individual-level (n = 29) OLS regression results showing the effect of NAcc and vmPFC activity on likeback ratings (from 1 to 7, with 7 being most likeable) in the fMRI sample. All models include participant age and self-rated attractiveness control variables.

	Accuracy	
Trained on:	Individual	Aggregate
Attractive	0.73	0.44
Career	0.52	0.23
Personality	0.61	0.18
Likeback	0.55	0.14
All	0.75	0.40
Chance:	0.50	0.10

Table 2.9. Comparing prediction accuracy between logistic regression models at the individual-level (binary choice) and OLS regression models at the aggregate-level (choice likelihood) using choice decomposition variables separately and combined for training in the in-lab sample. All models trained in 70% in-lab sample data and tested on 30% hold-out market data. Estimates are the average of 50 iterations.

	Individual-level Prediction Accuracy	
Trained on:	Within fMRI Sample	Market
Attractiveness	72.3	74.5
Career Prospects	57.1	51.1
Personality	69.1	65.6
Likeback	58.9	56.6
All Behavioral	76.7	75.7
NAcc	58.7	NA
vmPFC	58.3	NA
NAcc + vmPFC	58.7	NA
All Behavioral + NAcc	76.5	NA
All Behavioral + vmPFC	77.7	NA
All Behavioral + NAcc + vmPFC	77.5	NA
Chance:	50.0	50.0

Table 2.10. Comparing choice prediction accuracy between logistic regression models at the individual-level within the fMRI sample and in the simulated market data using choice decomposition variables and neural ROI separately and combined for training. All models trained in 70% fMRI sample data (i.e., market predictions trained on fMRI sample binary choice DV) and tested on 30% hold-out data. Classifiers were trained with 10-fold cross validation and accuracy estimates are the average of 50 iterations.

	Attractiveness	Career Prospects	Personality	Likeback	Attractiveness bin	Facial Expression	Age bin
Attractiveness							
Career Prospects	0.161						
Personality	0.552***	0.164					
Likeback	0.045	0.005	0.560***				
Attractiveness bin	-0.707****	-0.230	-0.528***	-0.165			
Facial Expression	-0.188	0.139	0.392*	0.486**	0		
Age bin	0.052	-0.148	-0.127	-0.107	0	0	
Profile Description	0.065	0.060	0.185	0.096	0	0	0
Note: n = 45					*p<0.05; **p<0.01; ***p<0.001; ****p<0.0001		

Table 2.11. Aggregate-level correlations between choice decomposition variables and factorial design elements in the in-lab sample.

	Attractiveness	Career Prospects	Personality	Likeback	Attractiveness bin	Facial Expression	Age bin	Profile Description	NAcc
Attractiveness									
Career Prospects	0.009								
Personality	0.493**	-0.041							
Likeback	-0.050	-0.053	0.546***						
Attractiveness bin	-0.739****	-0.201	-0.439**	-0.081					
Facial Expression	-0.208	0.080	0.274	0.364*	0				
Age bin	-0.051	-0.029	0.206	-0.129	0	0			
Profile Description	0.077	0.123	-0.037	0.044	0	0	0		
NAcc	0.673****	-0.103	0.364*	0.124	-0.410*	-0.150	-0.134	-0.018	
vmPFC	-0.024	0.191	0.105	0.375*	-0.132	0.145	0.040	-0.248	0.094

Note: n = 29 *p<0.05; **p<0.01; ***p<0.001; ****p<0.0001

Table 2.12. Aggregate-level correlations between choice decomposition variables and factorial design elements in the fMRI sample.

	Attractiveness	Career Prospects	Personality	Likeback	Attractiveness bin	Facial Expression	Age bin
Attractiveness							
Career Prospects	0.081						
Personality	0.707****	0.092					
Likeback	0.409*	-0.025	0.893****				
Attractiveness bin	-0.747****	-0.258	-0.611****	-0.414*			
Facial Expression	-0.194	0.044	0.318	0.510**	0		
Age bin	0.004	-0.006	0.100	0.140	0	0	
Profile Description	0.100	0.146	0.148	0.158	0	0	0
Note: n = 654							*p<0.05; **p<0.01; ***p<0.001; ****p<0.0001

Table 2.13. Aggregate-level correlations between choice decomposition variables and factorial design elements in the simulated market sample.

	Dependent variable:					
	Choice					
	Sample			Market		
Predictor (Aggregate Sample Means)	(1)	(2)	(3)	(4)	(5)	(6)
Attractiveness Ratings	0.331**		0.314**	0.255**		0.240**
	(0.022)		(0.036)	(0.038)		(0.058)
Career Prospects Ratings	0.030		0.064	−0.033		−0.032
	(0.016)		(0.050)	(0.028)		(0.081)
Personality Ratings	−0.041		−0.038	−0.025		−0.092
	(0.050)		(0.064)	(0.086)		(0.104)
Likeback Ratings	0.173**		0.118	0.100		0.086
	(0.057)		(0.066)	(0.098)		(0.107)
Attractiveness_bin (Medium)		−0.309**	−0.020		−0.191**	−0.013
		(0.062)	(0.031)		(0.048)	(0.050)
Attractiveness_bin (Low)		−0.398**	−0.021		−0.333**	−0.108
		(0.062)	(0.035)		(0.048)	(0.058)
Facial Expression (Smiling)		−0.040	0.014		−0.037	0.028
		(0.051)	(0.026)		(0.039)	(0.042)
Age (24-28)		−0.025	−0.031		0.016	0.008
		(0.051)	(0.020)		(0.039)	(0.032)
Profile Description (SES/Career)		−0.013	−0.044		−0.052	0.014
		(0.062)	(0.062)		(0.048)	(0.101)
Profile Description (Personality)		0.067	0.007		0.066	0.046
		(0.062)	(0.024)		(0.048)	(0.040)
R^2	0.951	0.625	0.959	0.782	0.654	0.834
Adjusted R^2	0.945	0.547	0.942	0.753	0.583	0.767
Residual Std. Error	0.053 (df = 31)	0.152 (df = 29)	0.054 (df = 25)	0.091 (df = 31)	0.118 (df = 29)	0.088 (df = 25)
F Statistic	149.981** (df = 4; 31)	8.058** (df = 6; 29)	57.835** (df = 10; 25)	27.735** (df = 4; 31)	9.146** (df = 6; 29)	12.534** (df = 10; 25)

Note: Market n = 654, Sample n = 45 *p<0.05; **p<0.01

Table 2.14. In-lab sample OLS regression results showing the effect of aggregate choice decomposition variables on in-lab sample aggregate choice likelihood and simulated market level aggregate choice likelihood (36 profiles).

	Dependent variable:					
	Choice					
Predictor (Aggregate Sample Means)	Sample			Market		
Atttractiveness	0.286**		0.230**	0.239**		0.232**
	(0.027)		(0.033)	(0.018)		(0.024)
Career Prospects	−0.026		−0.018	0.010		0.012
	(0.021)		(0.021)	(0.014)		(0.015)
Personality	0.032		0.046	0.033		0.034
	(0.049)		(0.046)	(0.033)		(0.034)
Likeback	0.147		0.107	0.103*		0.104
	(0.073)		(0.074)	(0.048)		(0.055)
NAcc		1.220**	0.368*		0.875**	0.049
		(0.182)	(0.137)		(0.170)	(0.102)
vmPFC		−0.016	−0.005		−0.011	−0.008
		(0.064)	(0.039)		(0.060)	(0.029)
R^2	0.87	0.58	0.89	0.91	0.45	0.91
Adjusted R^2	0.85	0.55	0.87	0.90	0.41	0.89
Residual Std. Error	0.09 (df = 31)	0.15 (df = 33)	0.08 (df = 29)	0.06 (df = 31)	0.14 (df = 33)	0.06 (df = 29)
F Statistic	50.34** (df = 4; 31)	22.63** (df = 2; 33)	40.34** (df = 6; 29)	79.07** (df = 4; 31)	13.26** (df = 2; 33)	49.86** (df = 6; 29)

Note: Market n = 654, Sample n = 29 *p<0.05; **p<0.01

Table 2.15. OLS regression results showing the effect of aggregate fMRI sample choice decomposition variables and neural ROIs on fMRI sample aggregate choice likelihood and simulated market level aggregate choice likelihood (n = 36 profiles).

	Dependent variable:					
	Likeback Ratings					
Predictor (Aggregate Sample Means)	Sample			Market		
Atttractiveness	−0.165**		−0.199**	−0.005		−0.008
	(0.060)		(0.072)	(0.042)		(0.055)
Career Prospects	−0.007		−0.022	−0.011		−0.013
	(0.052)		(0.050)	(0.036)		(0.039)
Personality	0.445**		0.413**	0.340**		0.335**
	(0.090)		(0.085)	(0.063)		(0.066)
NAcc		0.172	0.343		0.406	0.033
		(0.310)	(0.331)		(0.248)	(0.255)
vmPFC		0.250*	0.193*		0.055	0.031
		(0.110)	(0.088)		(0.088)	(0.068)
R^2	0.433	0.149	0.539	0.542	0.090	0.546
Adjusted R^2	0.380	0.097	0.462	0.499	0.035	0.470
Residual Std. Error	0.212 (df = 32)	0.256 (df = 33)	0.197 (df = 30)	0.148 (df = 32)	0.205 (df = 33)	0.152 (df = 30)
F Statistic	8.151** (df = 3; 32)	2.885 (df = 2; 33)	7.013** (df = 5; 30)	12.635** (df = 3; 32)	1.637 (df = 2; 33)	7.219** (df = 5; 30)
Note: Market n = 654, Sample n = 29						*p<0.05; **p<0.01

Table 2.16. OLS regression results showing the effect of aggregate fMRI sample choice decomposition variables and neural ROIs on fMRI sample aggregate likeback ratings and simulated market level aggregate likeback ratings (36 profiles).

	Aggregate-level Choice Prediction Accuracy		
Trained on:	In-lab Sample	Within fMRI Sample	Market
Attractiveness	36.5	32.2	35.8
Career Prospects	15.1	9.3	19.1
Personality	10.0	18.2	17.3
Likeback	14.4	7.3	13.4
All Behavioral	26.4	40.2	34.0
NAcc	17.6	21.3	32.5
vmPFC	14.7	10.0	15.8
NAcc + vmPFC	20.9	19.6	28.0
All Behavioral + NAcc	29.1	37.6	33.3
All Behavioral + vmPFC	25.6	36.9	31.8
All Behavioral + NAcc + vmPFC	30.9	36.0	30.7
Chance:	10.0	10.0	10.0

Table 2.17. Comparing choice prediction accuracy between OLS regression models at the aggregate-level (like rate) within the fMRI sample and in the in-lab sample and simulated market data using fMRI sample choice decomposition variables and neural ROI separately and combined for training. All models trained in 70% fMRI sample data (i.e., market predictions trained on fMRI sample aggregate choice likelihood DV) and tested on 30% hold-out data. Classifiers were trained with 10-fold cross validation and accuracy estimates are the average of 50 iterations.

CHAPTER III

Gene-Level Approaches to Genome-Wide Association: Developing Python-Based Tools for Gene-Level Association Testing

Genetic association studies have the potential to deepen our understanding of behavioral traits and tendencies studied in the social sciences (e.g., psychology, economics, consumer behavior). Advances in genetic sequencing technologies have allowed researchers to investigate genetic influences on a wide array of human behaviors. Indeed, research findings in social science genomics have reshaped how we think about risk taking (Aydogan et al., 2019), economic and political preferences (Benjamin et al., 2012), and even coffee consumption (Cornelis et al., 2015). At present, there are two primary methodologies that are used in genetic association studies: 1) the candidate gene approach, and 2) genome-wide association studies (GWAS).

Research using candidate genes has produced interesting insights across many domains. For example, in the dopamine receptor D4 variable number tandem repeat (DRD4 VNTR) is a well-studied candidate gene that has produced associations related to religiosity and prosociality (Sasaki et al., 2011), cultural value orientation (Kitayama et al., 2014), and postgame testosterone levels in salespeople following team-based games (Verbeke et al., 2015). In candidate gene studies, researchers restrict their analyses to a small number of genetic loci/ alleles, or a set of single nucleotide polymorphisms (SNPs) in a very small number of genes (i.e., often a single gene), and use sample sizes consistent with behavioral/ experimental research

studies (typically in the range of 200-500 per experiment). However, by limiting sample sizes and restricting analyses to a single variant, candidate gene studies limit their external validity and statistical power (Ioannidis, 2005, 2007; Chabris et al., 2012). Indeed, given that the true effect sizes for genetic aspects of complex social behaviors relevant to marketing are likely small, the sample sizes necessary to adequately power such studies are quite large.

On the other hand, GWAS occupy the opposite end of the methodological spectrum as a 'gold standard' for genetic association studies and have gained much traction among behavioral geneticists, psychiatrists, and genoeconomists (Benjamin et al., 2012). In GWAS, all of the SNPs from a SNP array (typically, in the order of millions of SNPs) are included in the analysis and alleles are tested to see if they occur more frequently at a certain level of the behavioral trait that is under investigation. However, given the single genetic variant level of analysis and massive number of variants being tests, performing a robust GWAS requires massive sample sizes (greater than 300,000), which is cost prohibitive in many settings (including, but not limited to business schools). For this reason, GWAS studies are largely only performed by large genetic consortia or labs with significant research grants. Additionally, the phenotypic or behavioral data that accompany large genetic databases feasible for use in a GWAS (e.g., the UK BioBank) are typically restricted to or primarily consist of medical and physiological characteristics. So, although GWAS is the gold standard for genetic association studies, conducting a proper, fully powered exploratory GWAS requires extensive resources and data. For these reasons, many researchers in marketing, psychology, and behavioral economics still use candidate gene approaches when studying the genetic underpinnings of complex psychological phenomenon (e.g., prosocial behavior or the endowment effect), even though such studies may be significantly underpowered and are known to produce false positives; it can be challenging to find dependent

variables that are interesting to marketers, psychologists, and behavioral economists in genetic datasets large enough to perform GWAS.

Researchers interested in genetic association studies who are well versed in experimental methods and who have primarily used candidate gene methods in the past, but are aware of their shortcomings and do not have the resources to run a proper GWAS, face many technical challenges when deciding to forego the candidate gene approach but continue studying genetic associations in their area of research. Consider the DRD4 VNTR, which has been showed to be involved in influencing the levels of dopamine uptake and transmission in the brain and/ or dopamine sensitivity in the brain (Wang et al., 2004). In candidate gene studies, DRD4 VNTR acts as a proxy measurement for variation in a larger number of genes that play a role in the dopaminergic signaling pathway. A candidate gene researcher may (reasonably) consider more precisely and directly measuring dopamine sensitivity by using genetic information from all genes involved in the dopaminergic pathway, rather than using the DRD4 VNTR as a proxy. Associations between this set of dopaminergic genes and the construct of interest could then be compared with associations between other genes and the construct of interest, with the expectation that the associations between dopaminergic genes would be significantly greater than other genes. However, from an individual researcher perspective the statistical tools necessary for implementing such a research design - a theory driven gene-level association comparison – are not publicly available, which makes this a very challenging design to implement for many researchers because of the sheer size of the genetic data and statistical problem (relative to the statistical tools necessary for candidate gene studies). That is, the statistical tools and expertise needed for such an approach are no longer similar to those necessary for candidate gene approaches, and, as such, the startup costs for such research are high (a similar argument can be

made for other approaches that are in middle of the candidate gene/ GWAS methodological spectrum as well).

The present research aims to develop a set of Python-based tools that researchers can use for gene-level hybrid approaches to genetic association methodologies, and provides initial demonstrations of these tools using data from the University of Michigan's Health and Retirement Study (HRS). Whereas the majority of exploratory genetic association studies are conducted at the SNP level of analysis, gene-level approaches have the ability to take advantage of two biological facts: 1) the known structure of genes/ mapping of genes in the genome, and 2) the likelihood of correlation based on the relative location of neighboring SNPs in the genome (i.e., SNPs that are closer together in the genome are more highly correlated). Rather than test the significance of individual SNPs (as in GWAS), or test several prespecified genetic variants (as in candidate gene studies), gene-level approaches utilize all of the observed information within a gene to test the association between this gene and the behavior/ trait of interest. The tools discussed in this chapter include three primary methods of genome-wide gene-level association analysis (i.e., three ways of representing a gene statistically): 1) unedited SNP data within a gene, 2) the creation of eigenSNPs using principal components analysis, and 3) representing a gene using factors from factor analysis. In the first approach, all of the observed SNPs within a gene are included in regression models to represent the gene. In the second approach, principal components are used to create eigenSNPs, from the SNPs observed within a gene, and these eigenSNPs are then used to represent the gene. After conducting a principal component analysis, the resulting orthogonal components (eigenvectors; or eigenSNPs) that explain >90% of the variance within a gene are then used in the model to represent higher order gene-level variation that exists between individuals. Similar to the eigenSNP approach, in the third approach, factor

analysis is conducted and the resulting factors are then used to represent the gene. In the eigenSNP and factor analysis approaches, these dimension reduction techniques are used to account for multicollinearity between SNPs within a gene, as well as create components/ factors that may represent higher order gene variants. Additionally, power analysis simulations of such dimension reduction techniques on genetic data have suggested that researchers can achieve higher statistical power in association studies by conducting analysis at the gene-level (Wang & Abbott, 2008; Shen & Zhu, 2009). That said, empirical tests of power analysis for gene-level association approaches are not yet present in the literature. As such, a primary contribution of this work is to provide Python-based tools for future research and testing of gene-level approaches.

Formally, the gene-level approaches discussed here can be modeled as separate regressions for each gene that are conducted using the model,

$$(1) \quad y_i = \mu + \beta_j x_{ij} + \varepsilon_i$$

where y_i denotes the value of the outcome variable for individual i, μ is the mean of the outcome variable in the population, x_{ij} denotes the minor allele/ pseudo-minor allele frequency of SNP/ eigenSNP/ factor j for individual i (under a minor allele dosage model), and ε_i is the residual or effect of exogenous factors on y_i. The slope coefficient for x_{ij}, β_j, is the unique effect of SNP/ eigenSNP/ factor j on y_i.

Of the gene-level approaches, the eigenSNP procedure has only been developed recently and is typically implemented in a manner more similar to the candidate gene approach (Set et al., 2014; Wang & Abbott, 2008; Shen & Zhu, 2009); researchers pick a handful of genes (less than

25) that they have theoretical reasoning to support their involvement in a given psychological or behavioral trait, and statistically test the effect of the entire gene on the given behavior. However, research funding/ investments into moderately sized genetic datasets such as the Health and Retirement Study (Health and Retirement Study, 2021) or Wisconsin Longitudinal Study (Herd, Doborah, and Roan, 2014), which have genetic samples (> 10,000) that are not large enough for GWAS, but have rich phenotypic data, may provide researchers with an opportunity to capitalize on the advantages of gene-level approaches, yet statistical tools for doing so are sparce or non-existent.

Whereas a traditional GWAS can be conducted relatively simply using genetic software packages such as PLINK (Purcell et al., 2007), to the best knowledge of this author (at the time of conducting this research), there is no software available for the creation of genome-wide gene-level associations and therefore no simple way for researchers to implement such procedures or similar gene-level approaches. Indeed, given the widespread availability and development of SNP-level association approaches (e.g., PLINK) it is possible that many researchers choose a SNP level of analysis despite an interest in gene-level associations, as technical and computations requirements for gene-level associations provide an additional barrier for such analyses.

Python Tools and Statistical Approach

This section describes the approach and functionality of the accompanied Python-based tools for gene-level genome-wide association analyses, which can be viewed and downloaded from GitHub at https://git.io/JRr5c.

The minimum data requirements for using the gene-level Python tools described in this chapter are: 1) a publicly available human genome reference build (such as hg19; NCBI, 2021)

and 2) a dataset that includes your dependent variable of interest, age and sex demographic information, and SNP-chip genetic data for all participants (such as the HRS or Wisconsin Longitudinal Study). All SNP-level quality control and preprocessing should be conducted prior to using these gene-level association tools, following standard SNP data quality control measures (e.g., SNPs with minor allele frequency greater than 5%, genotyping rate of greater than 1% per SNP, missingness of less than 5% for each individual, and a sample specific heterozygosity rate filter); this can be conducted in PLINK (Purcell et al., 2007). In Python, lazy loading of genetic data is conducted via the pandas-PLINK package (pandas-plink, 2021; a Python package that interfaces with PLINK). Lazy loading is necessary given the significant size of many genetic datasets, and, as such, allows SNP data to be loaded into memory for each gene, and gene-level association statistics to be computed, without the need to hold an entire genetic dataset in memory (and thus reducing the computation requirements for conducting gene-level association analyses). In short, the statistical process proceeds as follows: for each gene, SNP data is loaded, eigenSNPs/ factors are created using PCA/ factor analysis, and these SNP data/ eigenSNPs/ factors are subsequently used to represent each gene in regressions to determine association with the dependent variable of interest.

Given a SNP-level genomic dataset, the first task necessary for gene-level association is to identify and subset SNPs that are observed within a given gene, for all genes in the genome. This is accomplished by traversing genetic location information from a human genome reference build map of the human genome. For each gene, base pair start and end locations are given, which, along with SNP positioning data are used to tag genes that SNPs are located within. Once all observed genic SNPs are associated with a gene, these data and can be used to create gene representations with from SNP data. For PCA, eigenSNPs are created by running a PCA on the

SNP data within a given gene and extracting only the eigenvectors that explain 90% of the variance in the genetic data. Similarly, when representing a gene using factor analysis for dimension reduction, an exploratory factor analysis is run, without rotation, setting the number of dimensions equal to the number of SNPs observed within a given gene and recording the resulting number of factors that have an eigenvalue greater than 1. Then, a second factor analysis is performed, using promax rotation, and setting the number of factors equal to those with an eigenvalue greater than 1 from the initial exploratory factor analysis. For each gene, the resulting factors are used to represent this gene in subsequent association analysis.

Once data are loaded and processed at the gene-level, association analysis can proceed. Ordinary least squares (OLS) regression models are conducted in a similar manner to GWAS. Critically, rather than looking at a single SNP estimate in a regression model, treatment and control models need to be run and compared to isolate the effect of gene data while controlling for standard genome-wide study control variables. Using the minor allele dosage model described in Equation 1, the treatment model includes the SNP/ eigenSNP/ factor representation of the gene and control variables age, sex, and population stratification genetic controls, while the control model contains the same regressors but excludes the SNP/ eigenSNP/ factor representation of the gene. After running OLS on the treatment and control models, these models are then compared using a multiple partial F-test to extract the unique association of each gene with the dependent variable of interest (i.e., the overall effect of genetic variation within the gene on the dependent variable over and above the effect of control variables). As genes vary in the number of SNPs, and resulting eigenSNPs or factor representations, one cannot retrieve the associative contribution statistically with a single regression coefficient (as is the case with GWAS when retrieving test statistics from the SNP of interest).

For all genes across the genome, relevant association statistics can be extracted for each gene or a subset of genes (based on a list of gene names, chromosomes, and genomic positions). Additionally, the OLS function within the main association loop that is used to create association statistics can be easily be modified for use with different types of models and dependent variables (e.g., logistic regression/ binary dependent variables). Thus, summarizing the set of Python tools and statistical approach, each loop of the association function takes a gene, finds, subsets, and lazy loads the SNP data within that gene, creates eigenSNPs using PCA and factors using factor analysis as alternative representations of the gene, merges gene representation data back with the survey data, runs treatment and control regression models, compares regression results using a multiple partial F-test, and appends relevant gene-level association statistics to a results table prior to continuing on to the next gene in the genome mapping dataset (and this process is repeated for all ~20,000 genes in the human genome).

Empirical Demonstration and Testing

In this section, I provide a demonstration of how the Python tools discussed in this chapter can be used for gene-level association using data from the HRS.

Dataset

The HRS is a nationally representative longitudinal study that surveys approximately 20,000 individuals in the United States of America every two years. Data include rich individual and household-level information on health (e.g., cognitive functioning) and economic (e.g., income, assets) variables from individuals over 50 years of age. The HRS is a public dataset hosted by the Institute for Social Research (Survey Research Center) at the University of Michigan and sponsored by the National Institute on Aging and the Social Security Administration.

Between the years of 2006 and 2012, HRS collected genetic data from a significant subset (83% in 2006, and 84% in 2008) of the sample. Genetic data from HRS is stored by the National Center for Biotechnology Information's database of Genotypes and Phenotypes (dbGaP). The 2006 samples were collected using a mouthwash collection method, while the 2008 samples were collected using the Oragene DNA collection kit (OGR-250). All genotyping was conducted using the Illumina Human Omni-2.5 Quad beadchip (with 2.5 million SNP coverage) and performed by the National Institutes of Health (NIH) Center for Inherited Disease Research. Quality control of SNP genotyping was performed by the Genetics Coordinating Center at the University of Washington, Seattle, WA. A principal components analysis of the entire HRS genomic sample was conducted in PLINK, and the top four components are included in all association analyses to control for population stratification (Price et al., 2006).

For gene location and mapping, the International Human Genome Sequencing Consortium's hg19 homo sapiens genomic structural information was used. These data are publicly available and contain human genomic information including gene names, chromosome location, and start and end base pairs resulting from the Human Genome Project (NCBI36, 2021).

Variable Selection/ Phenotypes of Interest

Given that genetic associations with human behavior are of broad appeal across a wide variety of fields (from medicine to marketing), genetic association studies vary widely in the type of constructs that have been investigated. A key aspect of these variables is the extent that the variable is physiological (e.g., systolic blood pressure, diastolic blood pressure, waist-to-hip ratio), behavioral (e.g., smoking initiation, coffee consumption), or social-psychological (e.g., educational attainment, intelligence). Given the spectrum of variables that have been previously

studied in genetic association studies, it is important to determine how gene-level association techniques may vary in performance across phenotypes (such as the aforementioned physiological to social-psychological spectrum). As such, I have chosen to sample variables across the physiological to social-psychological spectrum for the following demonstration (Ebstein et al., 2010). Constructs identified for inclusion in this empirical demonstration of gene-level genome-wide association include: 1) body-mass-index (BMI), 2) depression (CESD), and 3) educational attainment (EDYRS; i.e., years of education). Being based on a combination of body measurements, BMI is the most physical/ biological of these constructs, whereas CESD, a key mental health disorder, is more psychological, and EDYRS more social-psychological.

Gene-level Association Descriptive Statistics and Comparisons

To illustrate preliminary characteristics of the associations produced by the genome-wide gene-level associations that may be conducted using the Python tools described in this chapter, output of these tools will be compared to an internal GWAS using HRS data for BMI, CESD, and EDYRS. Significance is tested using both a family-wide genome-wide significance threshold (i.e., 0.05/ number of statistical tests) and a static nominal significance threshold of 1×10^{-5}. The main association output provides similar test statistic results as a standard GWAS output, but at the gene-level. As such, many standard GWAS visualization tools can readily be used at the gene-level (e.g., Manhattan plotting tools).

BMI. An internal GWAS of BMI conducted 1,566,738 SNP associations and produced 0 genome-wide association and 29 nominal SNP associations (see Figure 3.1). Gene-level approaches, on the other hand, conducted 18,999 tests, and produced far fewer associations, with 1 genome-wide association using the SNPs within a gene method ("XIRP2") and nominal associations as follows: 4 genes when using all SNPs within a gene ("XIRP2", "EDIL3",

"HOXA2", "INA"; see Figure 3.2), 1 gene when using PCA and factor analysis ("HOXA2"; see Figure 3.3 and 3.4). Lambda values indicate that genomic inflation was lowest at the SNP-level of analysis ($\lambda = 1.06$), followed by gene-level approaches factor analysis ($\lambda = 1.18$), PCA ($\lambda = 1.28$), and SNPs within a gene ($\lambda = 1.58$; see Figure 3.5 for QQ plots).

CESD. An internal GWAS of CESD conducted 1,566,738 SNP associations and produced 1 genome-wide association ("rs77640966") and 34 nominal SNP associations (see Figure 3.6). Gene-level approaches, on the other hand, conducted 18,999 tests, and produced a single nominal association using the PCA approach ("DIS3L2"; see Figure 3.7 through 3.9 for Manhattan plots). Lambda values indicate that genomic inflation was lowest at the SNP-level of analysis ($\lambda = 1.06$), followed by gene-level approaches factor analysis ($\lambda = 1.24$), PCA ($\lambda = 1.25$), and SNPs within a gene ($\lambda = 1.59$; see Figure 3.10 for QQ plots).

EDYRS. An internal GWAS of EDYRS conducted 1,566,738 SNP associations and produced 1 genome-wide association ("rs2035444") and 68 nominal SNP associations (see Figure 3.11). Gene-level approaches, on the other hand, conducted 18,999 tests, and produced far fewer associations, with no genome wide association and nominal associations as follows: 0 genes when using all SNPs within a gene (see Figure 3.12), 1 gene when using PCA ("FTCDNL1"; see Figure 3.13) and 1 genes when using factor analysis ("FTCDNL1"; see Figure 3.14). Lambda values indicate that genomic inflation was lowest at the SNP-level of analysis ($\lambda = 1.04$), followed by gene-level approaches PCA ($\lambda = 1.15$), factor analysis ($\lambda = 1.16$), and SNPs within a gene ($\lambda = 1.33$; see Figure 3.15 for QQ plots).

Discussion

Datasets such as the Health and Retirement Study (HRS) have genetic samples that are significantly larger than typical candidate gene studies, are accessible to researchers around the

globe, and include a diverse range of rich phenotypic data of interest to social scientists across many fields, but are not large enough for traditional GWAS. Such genomic datasets may provide researchers with an opportunity to use statistical tools that capitalize on the advantages of gene-level association techniques (vs. SNP-level association techniques) but at this time gene-level association methods are understudied and the lack of publicly available tools to perform gene-level analyses may act as a barrier of entry to many researchers.

In this chapter, I discuss the development of a Python-based set of tools that can be used to implement genome-wide gene-level associations, and may subsequently be used to understand a variety of gene-level association techniques. These genome-wide gene-level association procedures combine a GWAS style whole-genome exploratory approach, but at the gene-level of analysis, rather than the SNP-level of analysis, and can be used to test the usefulness of gene-level approaches across research contexts and phenotypes.

By approaching genetic association from the gene-level, all available genic data is used to perform a whole-genome GWAS style statistical procedure, except with SNPs/ eigenSNPs/ factors within a gene, rather than individual SNPs. Across the genome in an exploratory analysis, such an approach thus reduces the total number of association tests from the number of SNPs (typically in the order of several million associations; ~2.5 million in the case of HRS) to the number of observed genes (typically in the order of tens of thousands of observed genes; humans have ~25,000 genes) and may hold the potential to reduce the sample size requirements necessary for adequate statistical power in a genetic association study of complex human behaviors. A preliminary demonstration of these genome-wide gene-level tools illustrates that gene-level associations tend to be more conservative and may reduce spurious associations, with fewer nominal gene association than SNP associations observed across three varied dependent

variables in the HRS. Additionally, after quality controlling data at the SNP level, some genomic inflation was observed in gene-level associations. That said, initial findings suggest that dimension reduction representations of a gene (such as PCA and factor analysis approaches) produce less genomic inflation than using all SNPs within a gene without any dimension reduction to represent the gene. Such tools could indeed be an initial step opening the door for social scientists to study gene-level associations in moderately sized, publicly available datasets, making genetic association research more accessible to a variety of researchers.

Limitations and Future Directions

Like all methodologies, gene-level association techniques are not without limitations. One of the most prominent current limitations of gene-level approaches is the issue of genic versus non-genic data. Gene-level approaches ignore non-genic data (i.e., SNPs that are not located within a gene). Although non-genic data was long thought to be 'junk DNA', not valuable for protein function and subsequent phenotypic variation, it is now clear that non-genic SNPs play a significant role in a wide variety of biological functions (Palazzo & Gregory, 2014; Gloss & Dinger, 2018). For example, the cleaned HRS data in this chapter contains ~ 1,604,118 SNPs, but when restricting data to genic SNPs, only ~ 714,886 SNPs are observed and used for analyses. Gene-level association approaches will need to develop parallel methodologies and statistical tools for incorporating non-genic genetic data.

Greater access to publicly available statistical tools for gene-level association will allow the development of further gene-level association methodologies. The tools presented in this chapter allow researchers to obtain gene-level association statistics for all genes across the genome, which can in turn be used to gain a further understanding of the statistical properties of gene-level tests (versus SNP-level tests) or test a wide variety of hypotheses. For example, a

researcher interested in dopaminergic genes may conduct empirical test either comparing the association strength between dopaminergic genes and a construct of interest with 1) associations between all other observed genes and the construct of interest, or 2) 'similar' genes that have similar length and number of SNP observations (among many other empirical testing possibilities). Having access to gene-level genome-wide association tools will also allow researchers to better understand the statistical properties of gene-level associations, beyond previous simulation work. Understanding the typical range of effect sizes garnered by gene-level approaches will allow researchers to conduct power calculations and develop scientifically robust standards for sample sizes necessary to study categories of behavioral traits and tendencies across fields. Finally, access to gene-level association tools may open the door for researchers to use existing genetic datasets to study a broad range of phenomena.

REFERENCES

Aydogan, G., Daviet, R., Linnér, R. K., Hare, T. A., Kable, J. W., Kranzler, H. R., Wetherill, R. R., Ruff, C. C., Koellinger, P. D., & Nave, G. (2019). Genetic Underpinnings of Risky Behavior Relate to Altered Neuroanatomy. *BioRxiv*, 862417.

Benjamin, D. J., & Cesarini, D. (2012). The genetic architecture of economic and political preferences. *Proceedings of the National Academy of Sciences of the United States of Ameirca, 109*(21), 8026-8031.

Chabris, C. F., Hebert, B. M., Benjamin, D. J., Beauchamp, J., Cesarini, D., van der Loos, M., Johannesson, M., Magnusson, P. K. E., Lichtenstein, P., Atwood, C. S., Freese, J., Hauser, T. S., Hauser, R. M., Christakis, N., & Laibson, D. (2012). Most Reported Genetic Associations With General Intelligence Are Probably False Positives. *Psychological Science*, *23*(11), 1314–1323.

Cornelis, M. C., Byrne, E. M., Esko, T., Nalls, M. A., Ganna, A., Paynter, N., Monda, K. L., Amin, N., Fischer, K., Renstrom, F., Ngwa, J. S., Huikari, V., Cavadino, A., Nolte, I. M., Teumer, A., Yu, K., Marques-Vidal, P., Rawal, R., … Chasman, D. I. (2015). Genome-wide meta-analysis identifies six novel loci associated with habitual coffee consumption. *Molecular Psychiatry*, *20*(5), 647-656.

Ebstein, R. P., Israel, S., Chew, S. H., Zhong, S., & Knafo, A. (2010). Genetics of Human Social Behavior. *Neuron* 65(6), 831–844.

NCBI. (2020) *GRCh38.p13 - Genome – Assembly.* Retrieved July 7, 2021, from https://www.ncbi.nlm.nih.gov/assembly/GCF_000001405.39

Gloss, B. S., & Dinger, M. E. (2018). Realizing the significance of noncoding functionality in clinical genomics. *Experimental & Molecular Medicine 2018 50:8*, *50*(8), 1–8.

Health and Retirement Study, public use dataset. Produced and distributed by the University of Michigan with funding from the National Institute on Aging (grant number NIA U01AG009740). Ann Arbor, MI, (2021).

Health and Retirement Study, restricted dataset. Produced and distributed by the University of Michigan with funding from the National Institute on Aging (grant number NIA U01AG009740). Ann Arbor, MI, (2021).

Herd, P., Deborah C., & Roan, C. (2014). Cohort Profile: Wisconsin Longitudinal Study (WLS). *International Journal of Epidemiology*, *43*, 34-41.

Ioannidis, J. P. A. (2005). Why Most Published Research Findings Are False. *PLOS Medicine*, *2*(8), e124.

Ioannidis, J. P. A. (2007). Non-Replication and Inconsistency in the Genome-Wide Association Setting. *Human Heredity*, *64*(4), 203–213.

Kitayama, S., King, A., Yoon, C., Tompson, S., Huff, S., & Liberzon, I. (2014). The Dopamine D4 Receptor Gene (DRD4) Moderates Cultural Difference in Independent Versus Interdependent Social Orientation. *Psychological Science*, *25*(6), 1169–1177.

NCBI36 - hg18 - Genome - Assembly - NCBI. (n.d.). Retrieved April 19, 2021, from https://www.ncbi.nlm.nih.gov/assembly/GCF_000001405.12/

Palazzo, A. F., & Gregory, T. R. (2014). The Case for Junk DNA. *PLoS Genetics*, *10*(5), e1004351.

Pandas-plink's documentation — pandas-plink 2.2.9 documentation. (n.d.). Retrieved July 7, 2021, from https://pandas-plink.readthedocs.io/en/latest/

PLINK: Whole genome data analysis toolset. (n.d.). Retrieved April 19, 2021, from https://zzz.bwh.harvard.edu/plink/contact.shtml

Price, A. L., Patterson, N. J., Plenge, R. M., Weinblatt, M. E., Shadick, N. A., & Reich, D. (2006). Principal components analysis corrects for stratification in genome-wide association studies. *Nature Genetics*, *38*(8), 904–909.

Purcell, S., Neale, B., Todd-Brown, K., Thomas, L., Ferreira, M. A. R., Bender, D., Maller, J., Sklar, P., De Bakker, P. I. W., Daly, M. J., & Sham, P. C. (2007). PLINK: A tool set for whole-genome association and population-based linkage analyses. *American Journal of Human Genetics*, *81*(3), 559–575.

Sasaki, J. Y., Kim, H. S., Mojaverian, T., Kelley, L. D. S., Park, I. Y., & Janušonis, S. (2011). Religion priming differentially increases prosocial behavior among variants of the dopamine D4 receptor (DRD4) gene. *Social Cognitive and Affective Neuroscience*, *8*(2), 209–215.

Set, E., Saez, I., Zhu, L., Houser, D. E., Myung, N., Zhong, S., Ebstein, R. P., Chew, S. H., & Hsu, M. (2014). Dissociable contribution of prefrontal and striatal dopaminergic genes to learning in economic games. *Proceedings of the National Academy of Sciences of the United States of America*, *111*(26), 9615–9620.

Shen, Y. F., & Zhu, J. (2009). Power analysis of principal components regression in genetic association studies. *Journal of Zhejiang University: Science B*, *10*(10), 721–730.

Verbeke, W. J. M. I., Belschak, F. D., Bagozzi, R. P., & De Rijke, Y. B. (2015). Postgame testosterone levels of individuals in team-based status games are affected by genetic makeup, gender, and winning versus losing. *Journal of Neuroscience, Psychology, and Economics*, *8*(3), 135–159.

Wang, K., & Abbott, D. (2008). A principal components regression approach to multilocus genetic association studies. *Genetic Epidemiology*, *32*(2), 108–118.

Wang, E., Ding, Y.-C., Flodman, P., Kidd, J. R., Kidd, K. K., Grady, D. L., Ryder, O. A., Spence, M. A., Swanson, J. M., & Moyzis, R. K. (2004). The Genetic Architecture of Selection at the Human Dopamine Receptor D4 (DRD4) Gene Locus. *American Journal of Human Genetics*, *74*(5), 931-944.

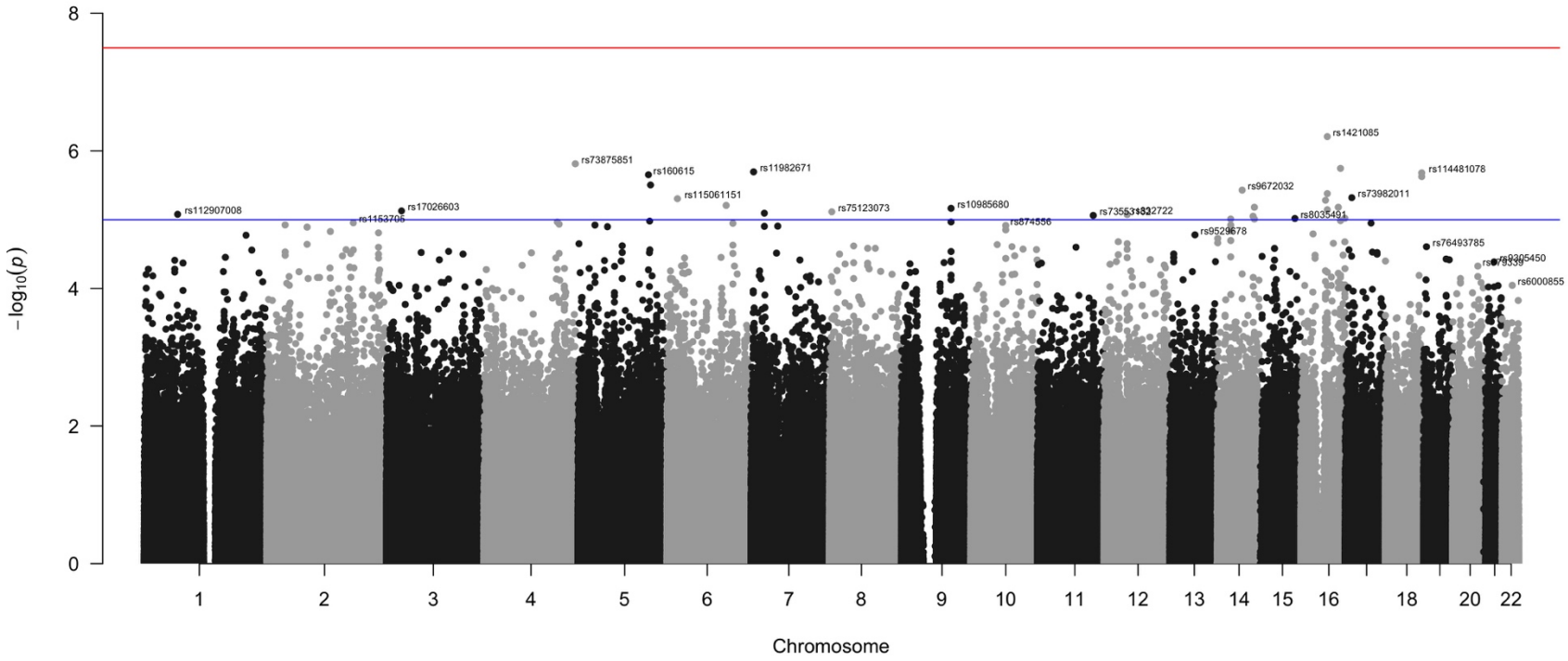

Figure 3.1. Manhattan plot for SNP associations with BMI resulting from GWAS using HRS data.

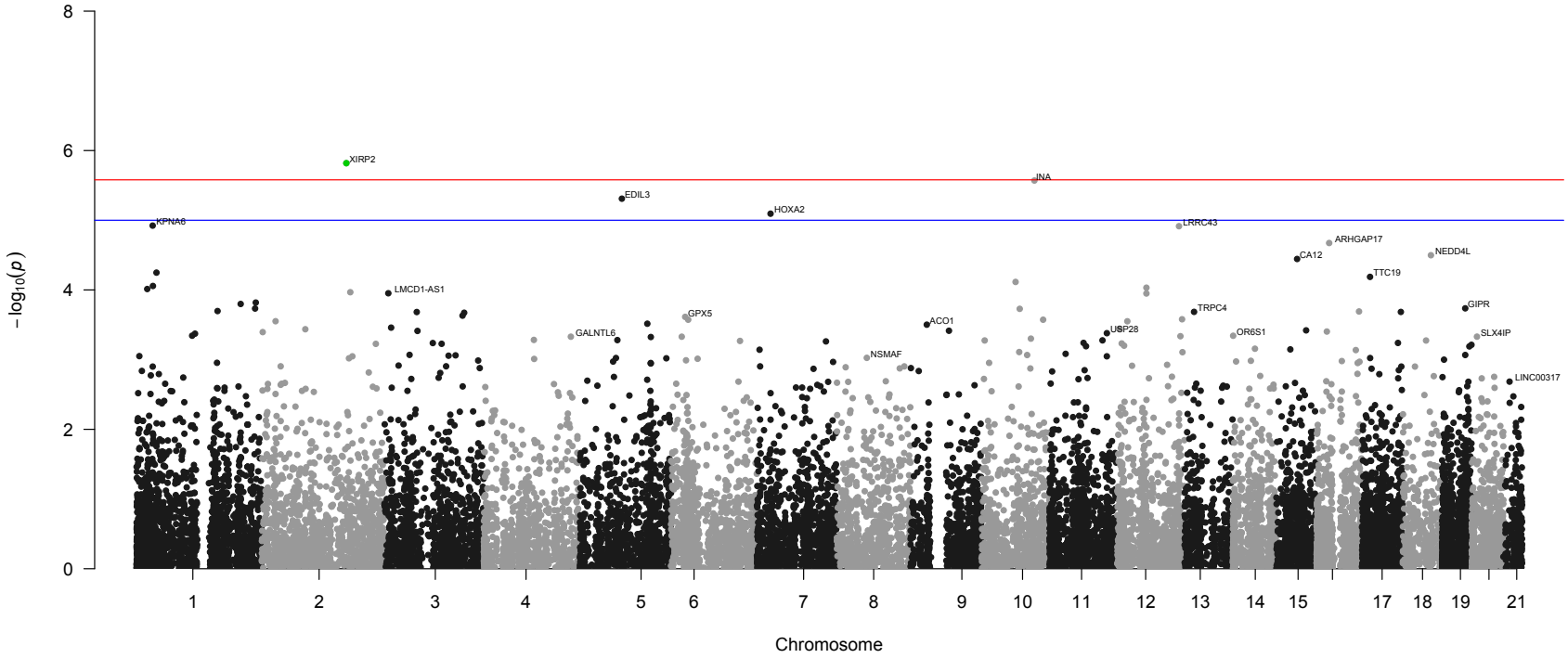

Figure 3.2. Manhattan plot for gene associations with BMI resulting from gene-level analysis using all SNPs within each gene observed in the HRS data.

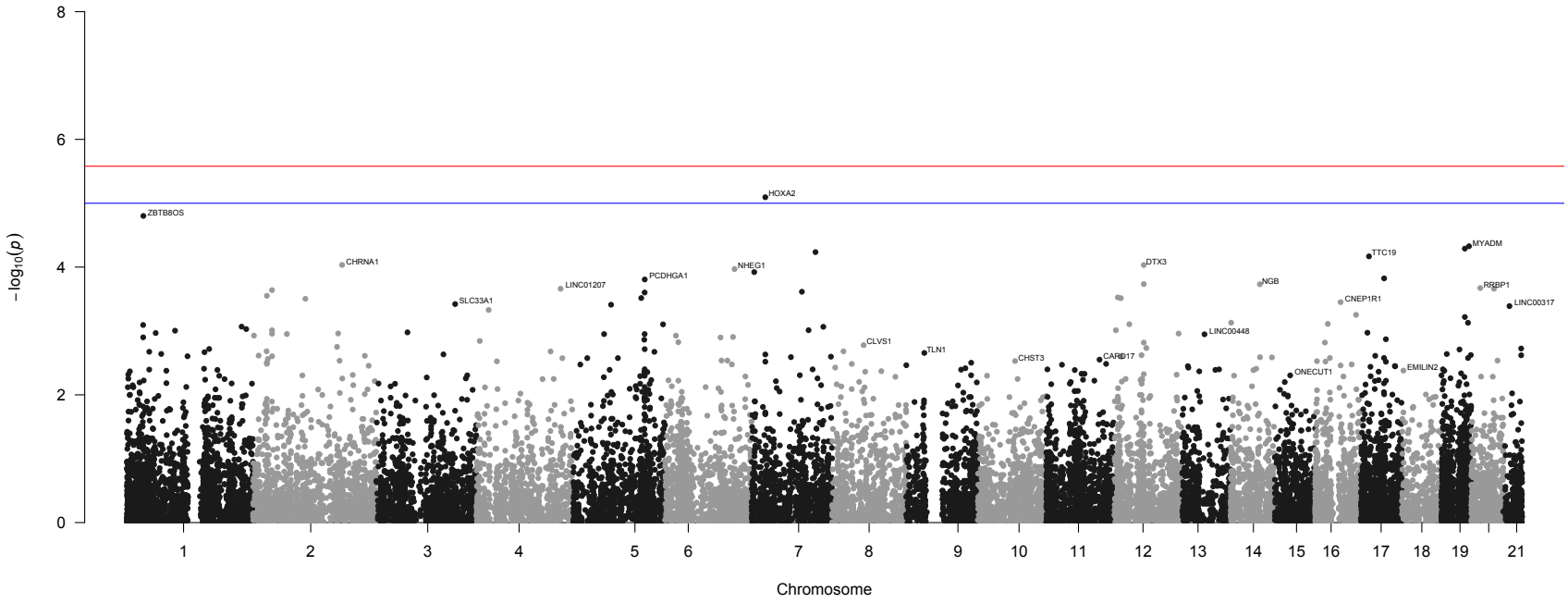

Figure 3.3. Manhattan plot for gene-level associations with BMI resulting from PCA analysis using SNPs within each gene observed in the HRS data.

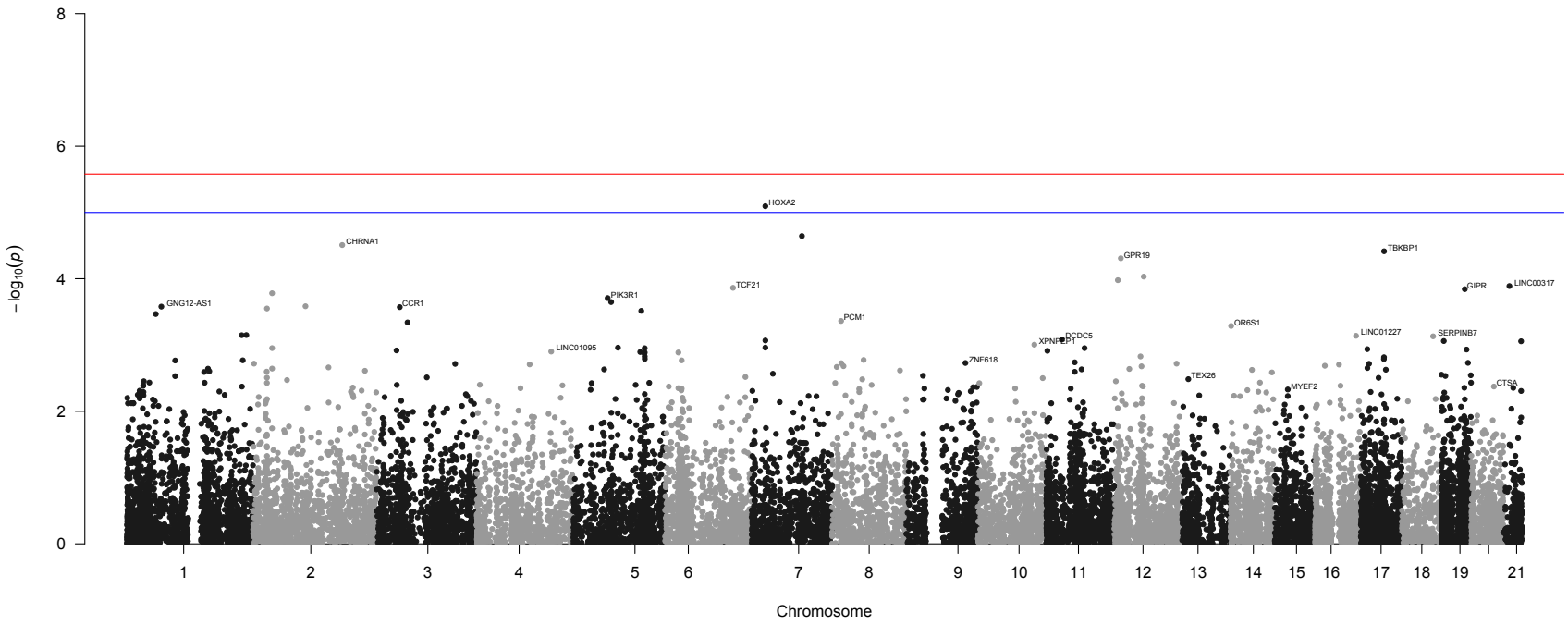

Figure 3.4. Manhattan plot for gene-level associations with BMI resulting from factor analysis using SNPs within each gene observed in the HRS data.

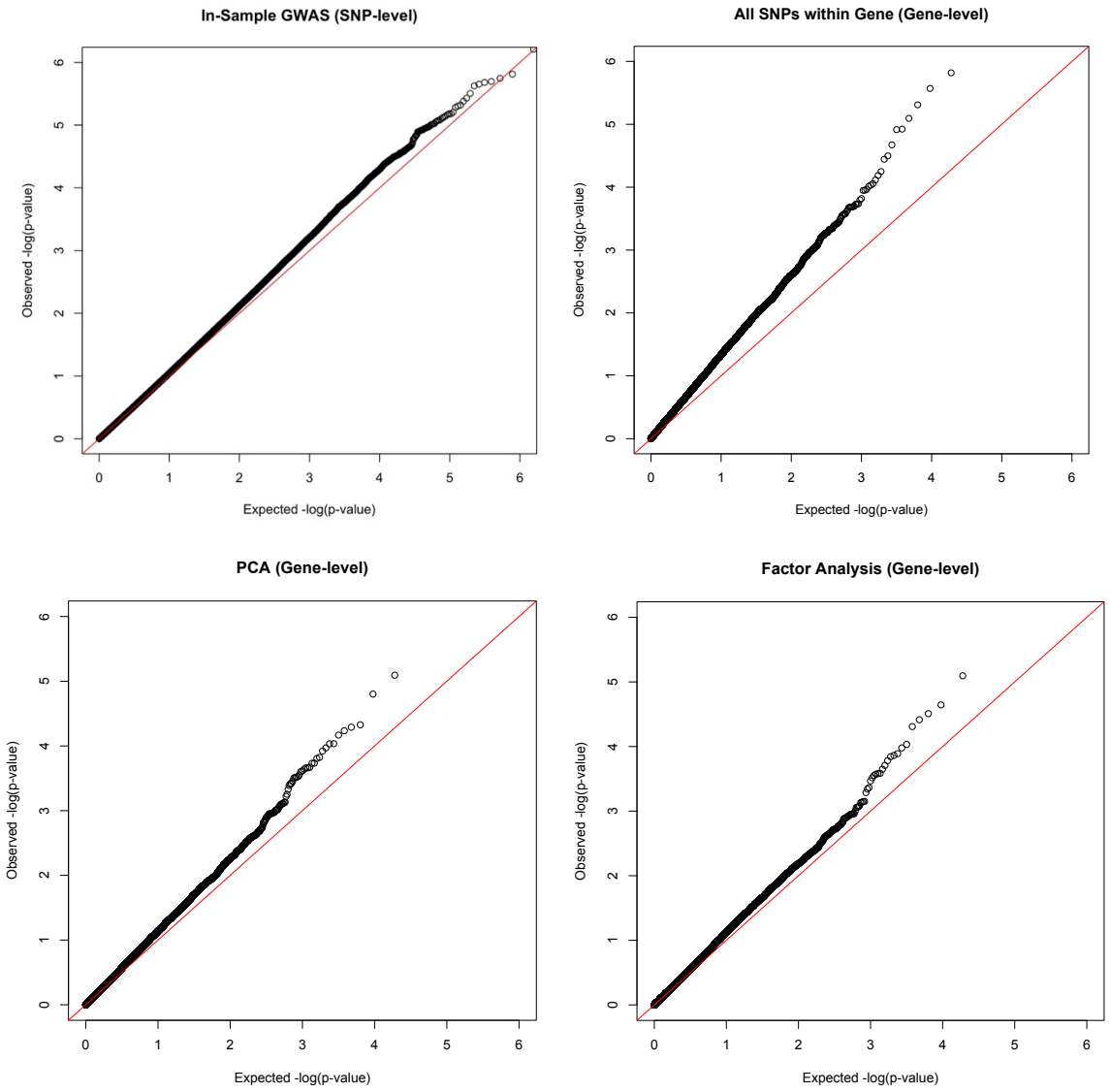

Figure 3.5. QQ plots showing genomic inflation for genetic associations with BMI using various association methods using data from the HRS.

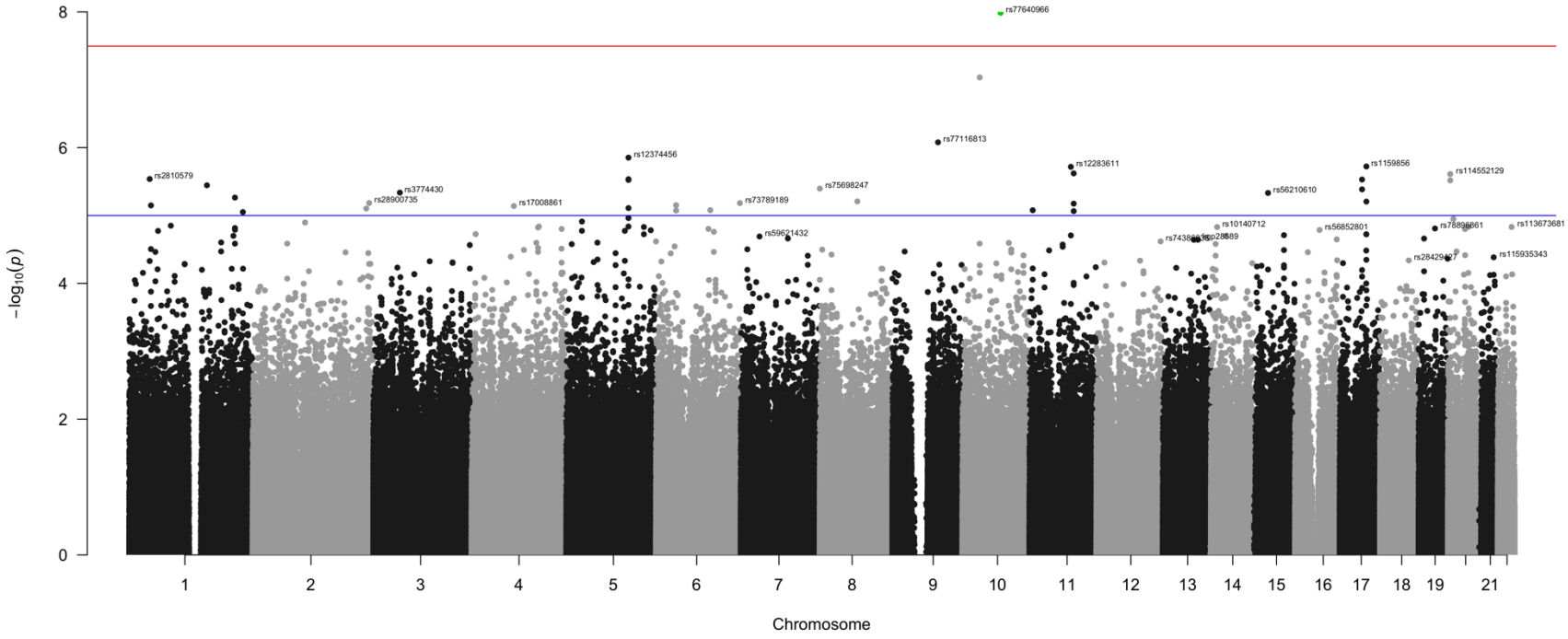

Figure 3.6. Manhattan plot for SNP associations with CESD resulting from GWAS using HRS data.

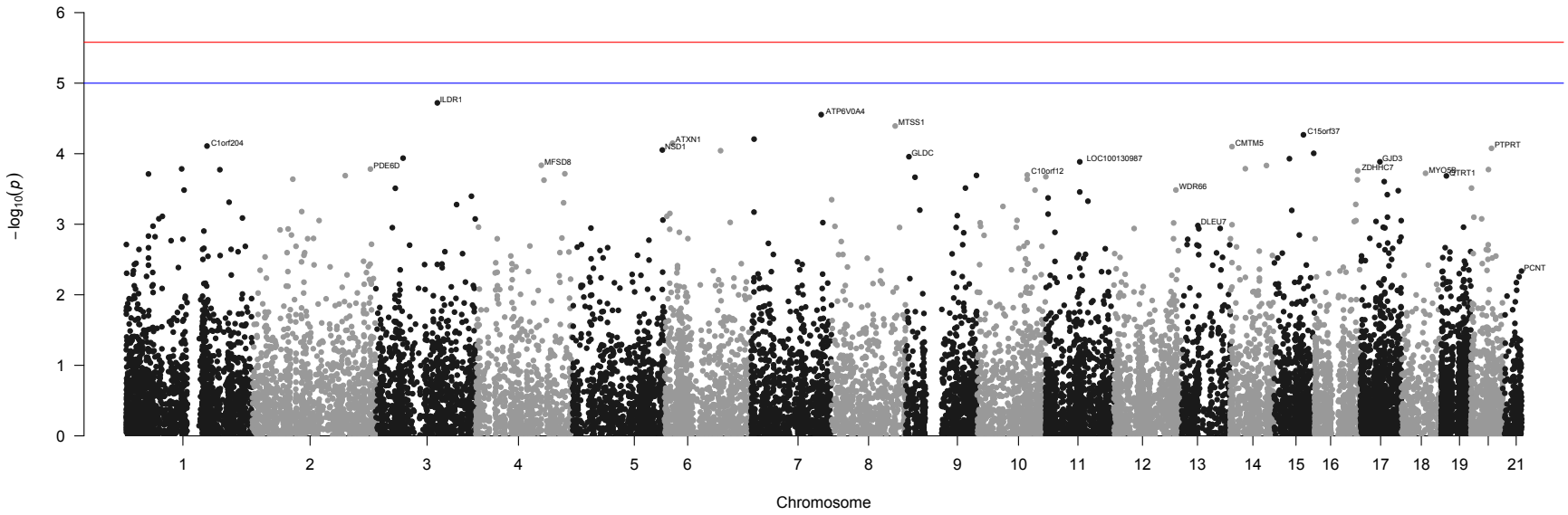

Figure 3.7. Manhattan plot for gene associations with CESD resulting from gene-level analysis using all SNPs within each gene observed in the HRS data.

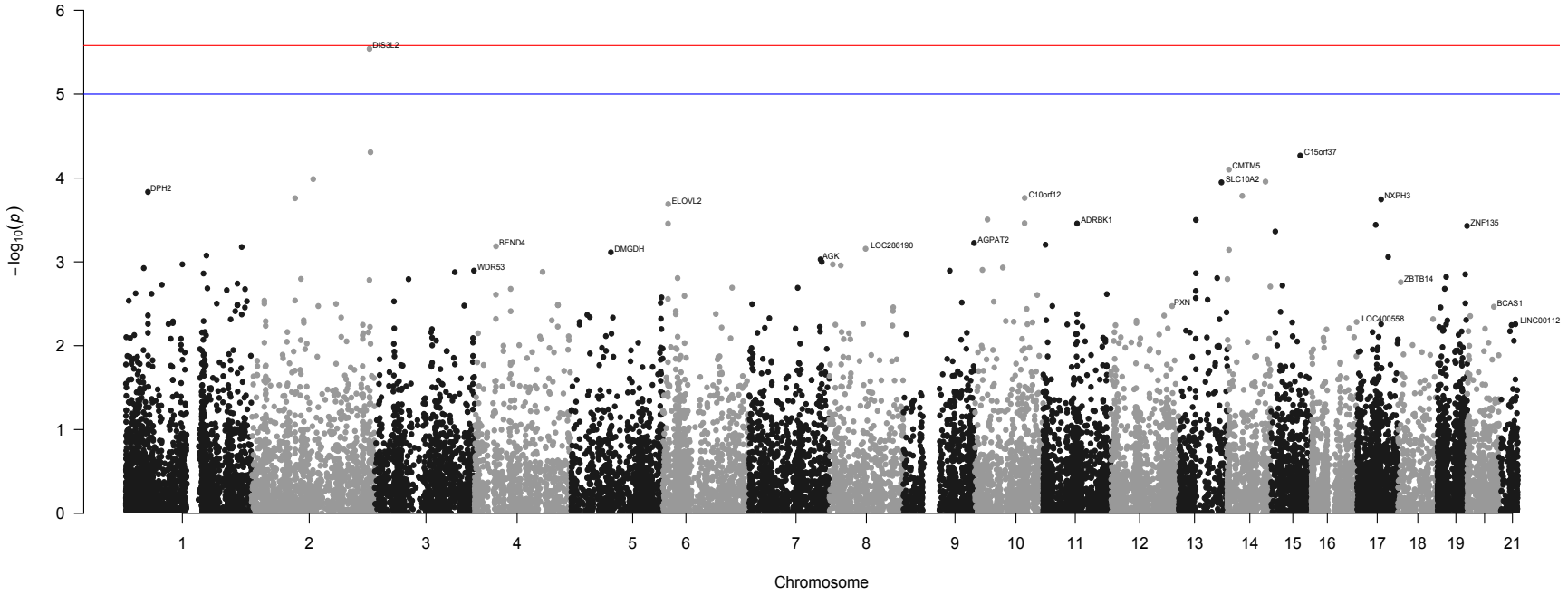

Figure 3.8. Manhattan plot for gene-level associations with CESD resulting from PCA analysis using SNPs within each gene observed in the HRS data.

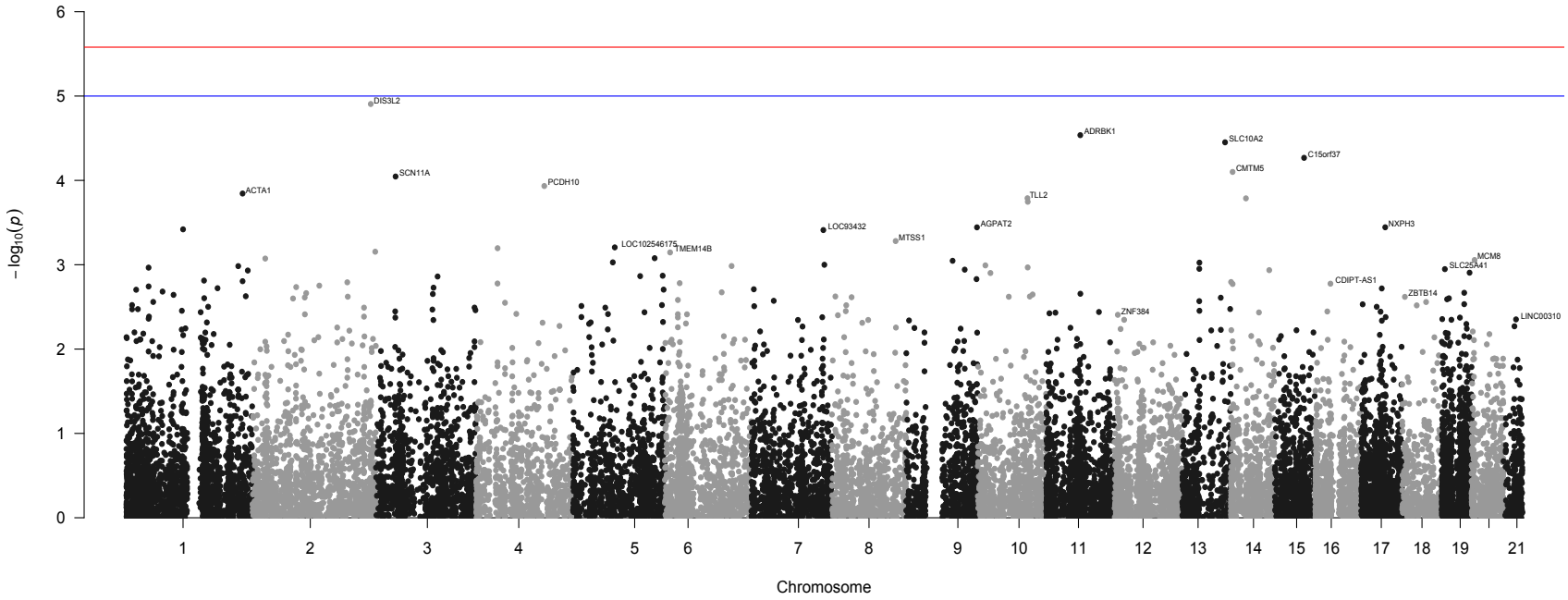

Figure 3.9. Manhattan plot for gene-level associations with CESD resulting from factor analysis using SNPs within each gene observed in the HRS data.

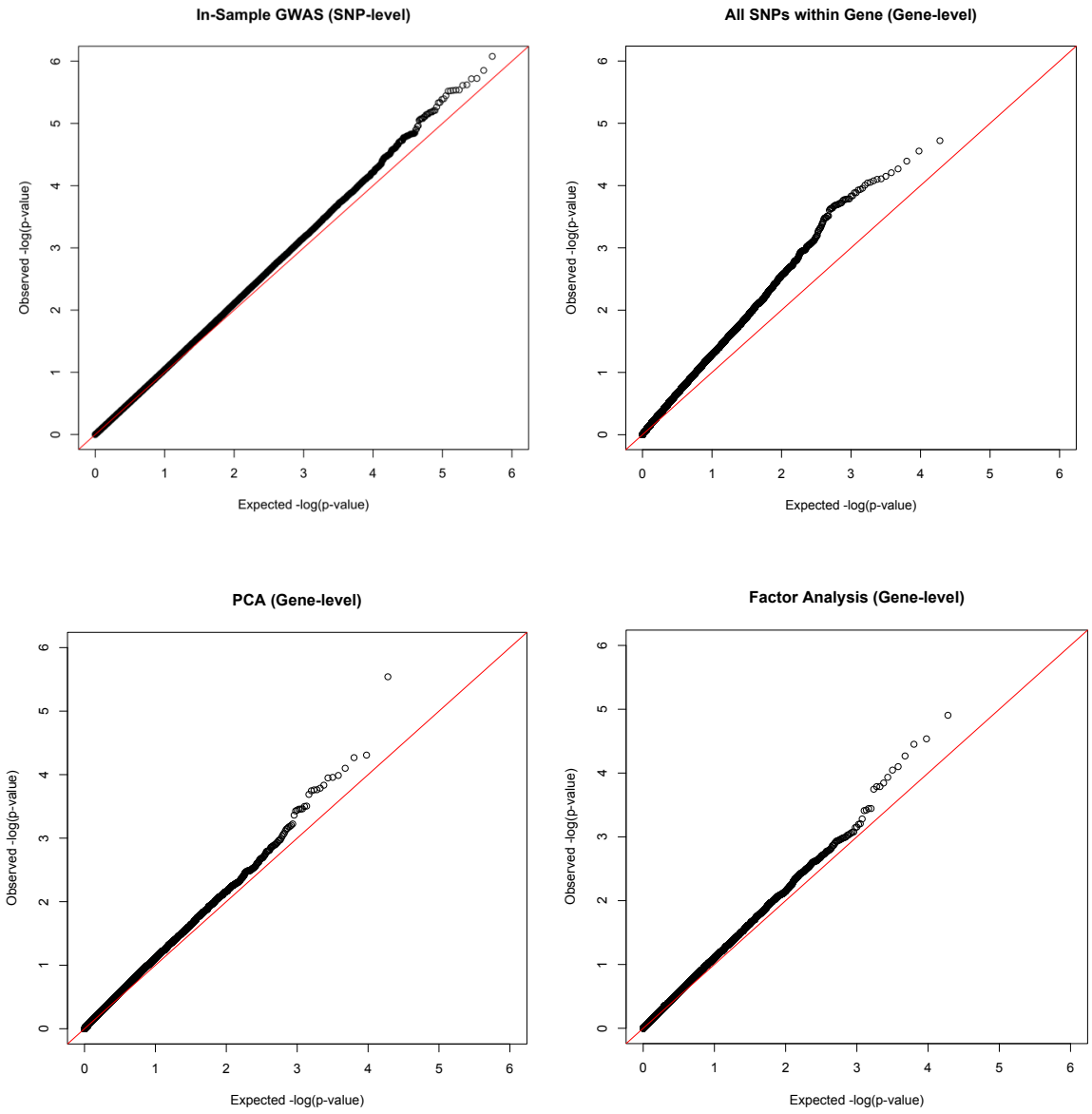

Figure 3.10. QQ plots showing genomic inflation for genetic associations with CESD using various association methods using data from the HRS.

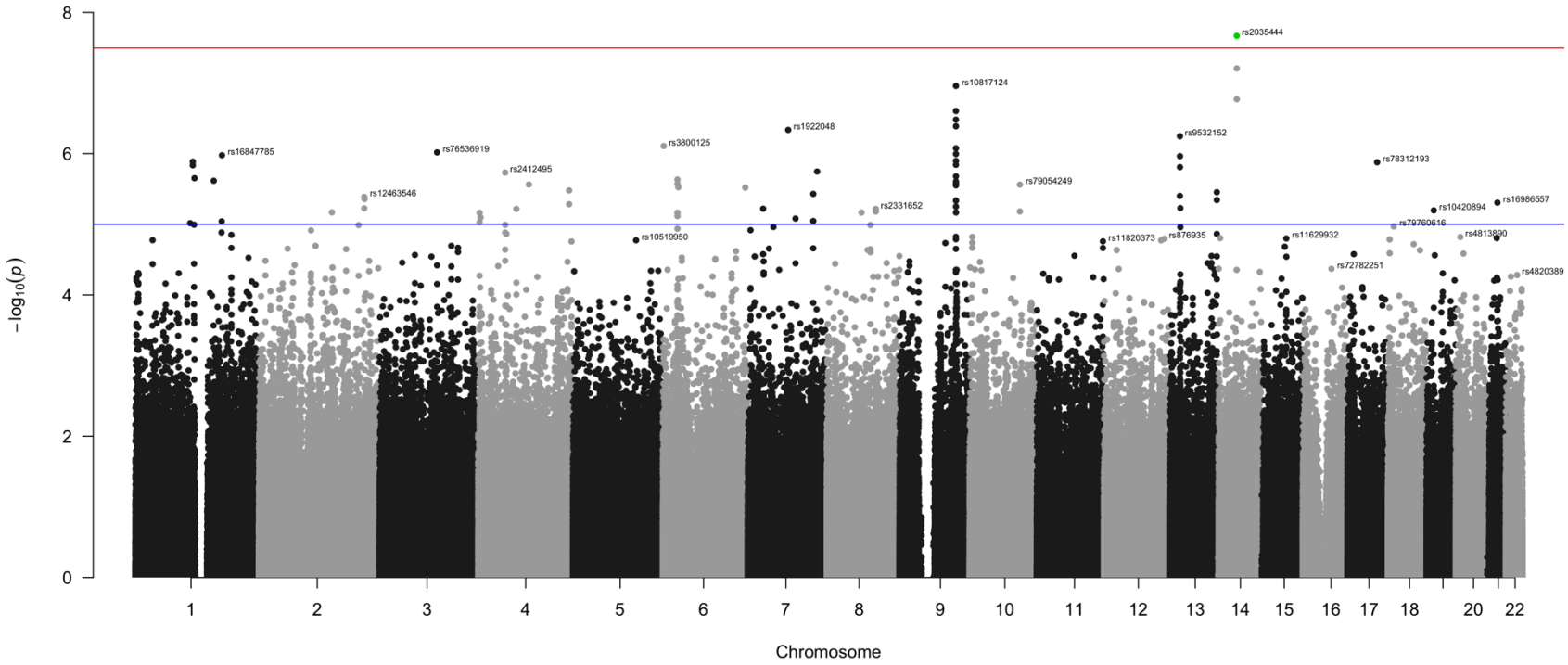

Figure 3.11. Manhattan plot for SNP associations with EDYRS resulting from GWAS using HRS data.

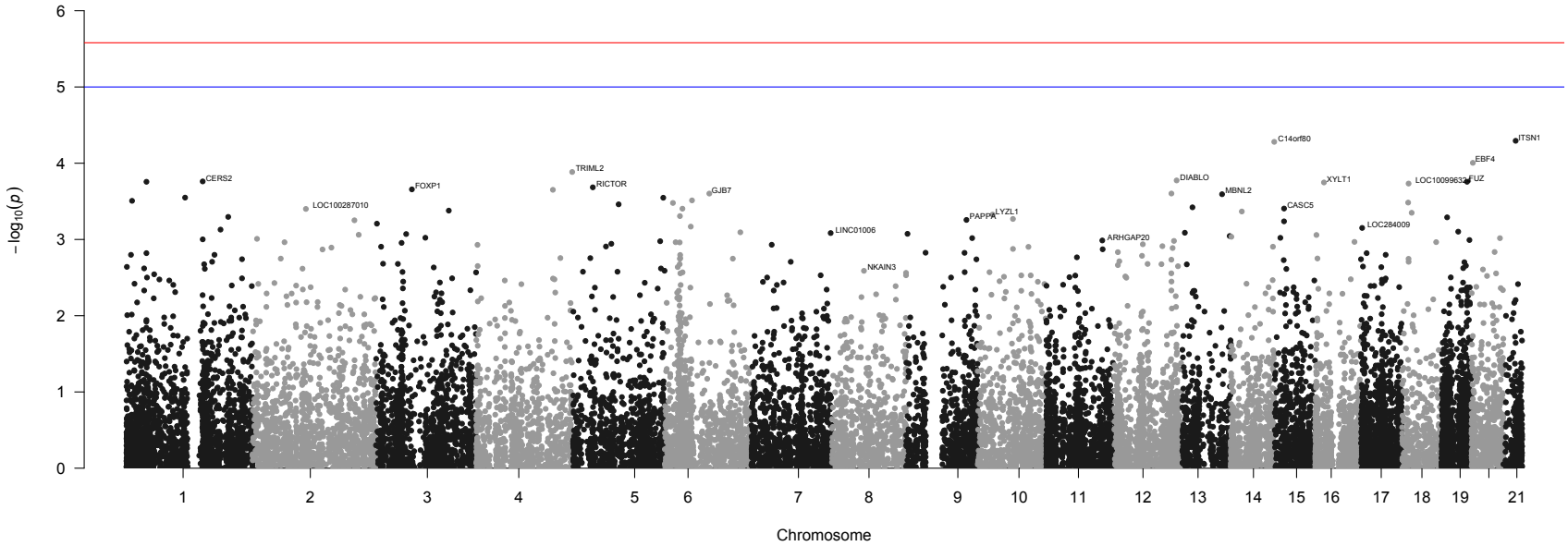

Figure 3.12. Manhattan plot for gene associations with EDYRS resulting from gene-level analysis using all SNPs within each gene observed in the HRS data.

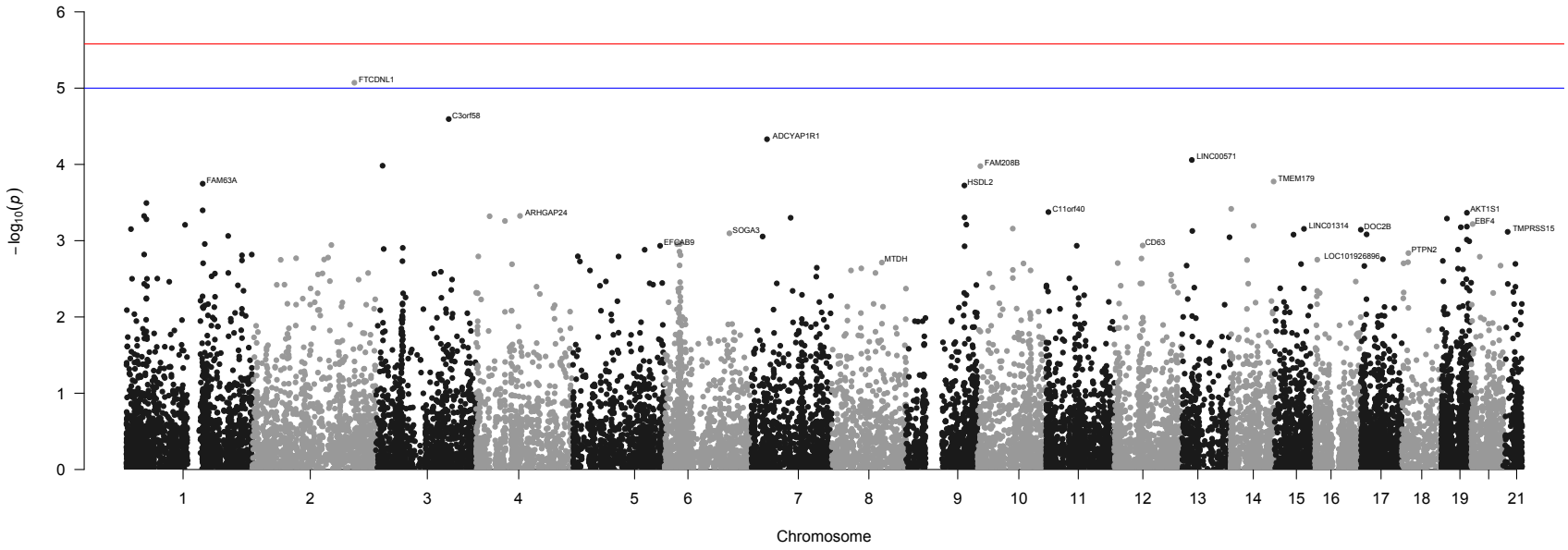

Figure 3.13. Manhattan plot for gene-level associations with EDYRS resulting from PCA analysis using SNPs within each gene observed in the HRS data.

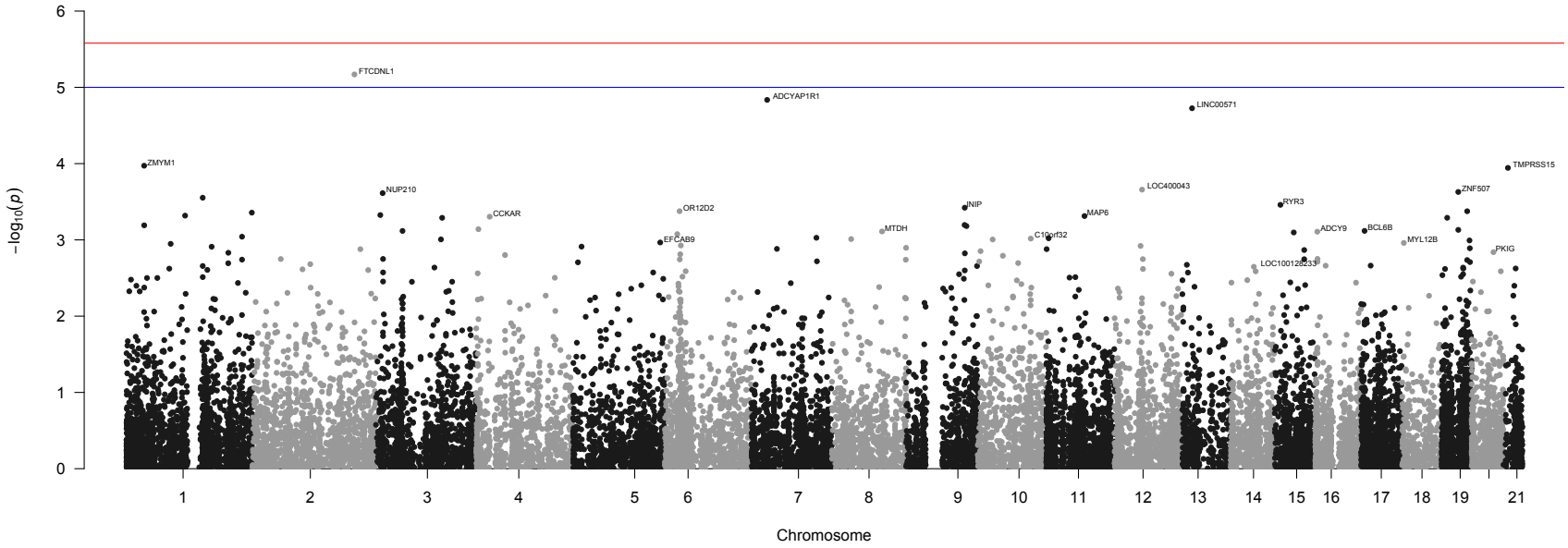

Figure 3.14. Manhattan plot for gene-level associations with EDYRS resulting from factor analysis using SNPs within each gene observed in the HRS data. Note: due to computational resource limitations, only chromosome 1 and 2 are displayed at this time.

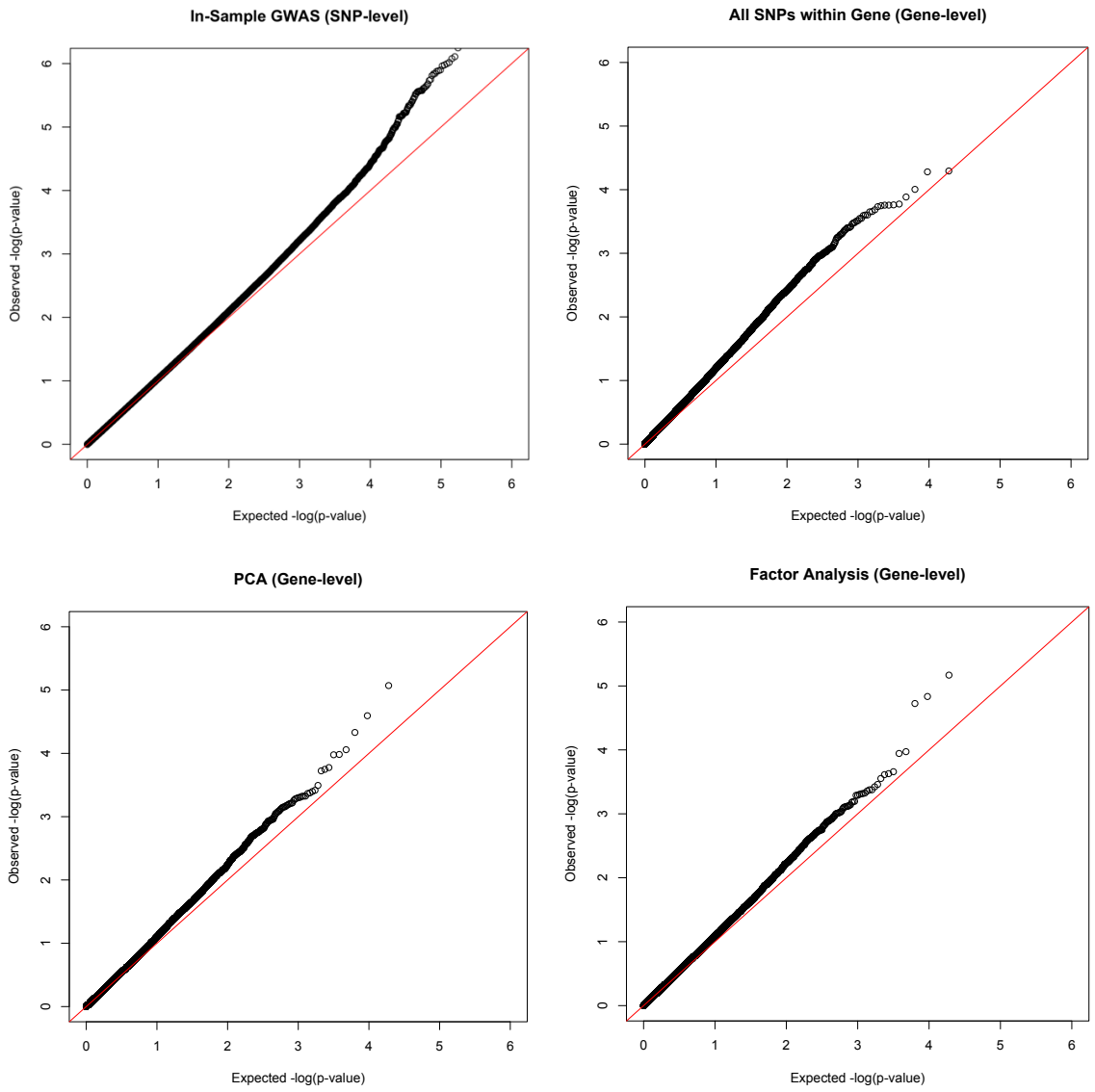

Figure 3.15. QQ plots showing genomic inflation for genetic associations with EDYRS using various association methods using data from the HRS.